Differential effects of target height on immediate and delayed pointing actions: an ERP study

by

Rayan Moukhaiber

A thesis submitted in partial fulfillment of the requirements for the degree of

Master of Science

Neuroscience
University of Alberta

Abstract

Visually guided actions are those that are completed using available visual information, such as reaching for a cup of coffee while looking at it. In the absence of visual information, our hand actions are guided by previously stored visual information; these are known as memory-guided actions. Naturally, memory-guided actions are less accurate and slower than visually guided actions. Existing neuropsychological literature has proposed that immediate, visually guided actions are controlled by dorsal-visual stream processes in the parietal cortex, whereas delayed, memory-guided actions are reliant on ventral-visual stream processes in the inferior temporal cortex. It has been shown that the N170, an event-related potential (ERP) component linked to perceptual processes associated with object and face recognition and memory, also reflects processing needed for delayed actions to remembered targets. However, the greater part of studies investigating the N170 ERP, have used experimental paradigms reliant on actions conducted within the lower visual field. This is understandable given the fact that a significant portion of behaviours are conducted within the lower visual field, including typing on a keyboard or reaching for a cup of coffee. The present experiment measured the N170 ERP as a function of the height of a target to-be-reached-to, in order to determine how stimulus locality in the upper and lower visual fields will affect immediate and delayed actions. We hypothesized that if delayed actions require more perception-based processes compared to immediate actions, they will also differ between target locations in the upper and lower visual fields. That is, delayed actions to targets in the upper visual field may be more perceptually taxing, take longer to execute, and be associated with a greater amplitude N170. Right-handed participants (N=28) were instructed to, reach out and touch a black target appearing on a touchscreen monitor in front of them, whenever they heard an auditory cue. The experiment consisted of two conditions, an immediate condition, and a delayed condition. The two conditions differed in timing by an average of 350 milliseconds. This has been shown in the literature to significantly alter behavioral and neural processing for targets in the lower visual field. The target location was manipulated so that targets can appear anywhere in the upper and lower visual field while simultaneously recording behavioral and electroencephalography (EEG) data. Our results indicated that memory-guided actions were initiated faster than visually guided actions but the two conditions were equivalent in terms of accuracy and movement time. Moreover, the N170 ERP exhibited a greater difference between conditions in the left hemisphere versus the right hemisphere, which replicates previous visuomotor literature. Contrary to our hypothesis, there was not an interaction between reach-height and either reaching type. This suggests that hand-arm kinematics and the neural circuitry underlying visually- and memory-guided actions may be relatively unchanged for targets in the upper visual field.

Preface

This thesis is an original work by Rayan Moukhaiber. No part of this thesis has been published previously. The research project, of which this thesis is a part, received research ethics approval from the University of Alberta Research Ethics Board, Project Pro00014392.

Dedication

I dedicate this thesis to my parents, Walid and Randa.

Acknowledgements

First and foremost, I would like to thank my supervisors Drs. Anthony Singhal and Jeremy Caplan for always supporting me in my program and pushing me to be the best version of myself. Under your guidance, I have changed for the better and become a better researcher.

In addition, I would like to extend my appreciation for my supervisory committee Drs. Sandra Wiebe and Craig Chapman. I would also like to acknowledge that my research work would not have been possible without the scholarship support I received from the QEII graduate award. I would like to personally thank Dr. Reyhaneh Bakhtiari and PhD Candidate Sucheta Chakravarty, for all of your insight and programming assistance throughout the duration of the Masters. Thank you to my parents, Walid and Randa, my brothers Gabby and Liam, and my cousin Shadi. You all reminded me to never take life too seriously and were patient and kind enough to constantly entertain my graduate ramblings. Lastly, Cal and Jan, Taylor, Bernie and Bella, I hope you all know that you have profoundly impacted me and that I could not have done this without any of you.

Table of Contents

List of Tables

List of Figures

List of Symbols and Abbreviations

Perception-Action Model	**PAM**
Initiation Time	**IT**
Movement Time	**MT**
Pointing Accuracy	**PA**
Milliseconds	**ms**
Microvolts	**µV**
Event-Related Potential(s)	**ERP / ERPs**
Electroencephalography	**EEG**
Lateral Occipital Cortex	**LOC**
Lateral Occipital Sulcus	**LOS**
Inferior Temporal Sulcus	**ITS**
Anterior Intraparietal Sulcus	**aIPS**
Functional Magnetic Resonance Imaging	**fMRI**
Transcranial Magnetic Stimulation	**TMS**

Appendices

Chapter 1:

Background and Design of Current Study

Rayan Moukhaiber[1], Anthony Singhal[1,2], Jeremy B. Caplan[1,2], Leanna C. Cruikshank[1]

[1]Neuroscience and Mental Health Institute, University of Alberta

[2]Department of Psychology, University of Alberta

1.0 Introduction

The simple act of reaching out and grabbing a cup of coffee in the morning, is a consequence of the interplay between the sensory system and the motor system. Conveniently, the interaction between these two systems has been labeled ‘sensorimotor integration’ as it encompasses the input of sensory information from multiple sources that lead to the output of a voluntary motor movement (Machado et al., 2010). The notion of sensorimotor integration has led to the systematic investigation of skilled motor acts, their neural substrates, and the establishment of what is now known as the Perception-Action Model (PAM; Goodale & Milner, 1992). This model suggests that there is a double dissociation between dorsal and ventral visual streams originating from the primary visual cortex (Mishkin et al., 1983), and that these visual pathways facilitate distinct reaching types (Goodale, 2014). Considerable evidence suggests that the dorsal stream is tasked with transforming real-time visual information and informing the motor system to produce a skilled motor act, while the ventral stream is understood to facilitate with actions in the absence of vision through accessing stored perceptual information (Goodale, 2014). One research group investigating these hand actions, not only demonstrated there are differences between these reaching types, but that electrophysiological recordings could also be used to measure these differences (Cruikshank et al., 2012a). The purpose of my experiment is to build on and extend the foundation laid down by Cruikshank et al. (2012a), by integrating a height element into their goal-directed reaching task. By manipulating the stimulus location across both the lower and upper visual fields, I sought to elucidate the influence this may have on the perceptual and biomechanical demands of immediate and delayed actions. Kinematic data was logged including standard reported measures such as, initiation time, movement time and overall accuracy. In addition, electrophysiological activity was recorded following a movement initiation cue, but prior to movement initiation using the same event-related potential (ERP) marker first introduced by Cruikshank et al. (2012a).

1.1 Two-visual Pathways Hypothesis

One of the earliest accounts of two-visual pathways, was by Schneider (1969) who found that when severing the superior colliculi of Syrian Golden Hamsters, they could identify but no longer direct themselves towards an object. On the other hand, when the ablation revolved around more posterior areas, such as the visual cortex, these animals presented with the exact opposite pattern of deficits. He postulated that these two kinds of visual effects hinted towards the existence of two distinct visual processing areas, such that superior colliculi mechanisms are responsible for object localization (i.e., where is the object?) and visual cortex mechanisms in charge of object identification (i.e., what is the object?). This distinction between ‘what’ and ‘where’ processing of objects was significant, as it established a preliminary framework for other research efforts to investigate this phenomenon. Over a decade later, Mishkin et al. (1983) attempted to reconcile the recent discoveries of the animal neuropsychological literature and provide a re-interpretation of the object identification/object localization hypothesis. Utilizing Rhesus Macaques as an animal model this time around, their methodology remained identical to Schneider (1969) in that they were removing cortical matter and subsequently recording any observed deficits. Via bilateral extraction of the inferior temporal cortex of Rhesus monkeys, they found that these monkeys seemingly lost their ability to identify objects, yet their object localization was still intact. Interestingly, the Rhesus monkeys presented with an inverse pattern of deficits if the inferior parietal cortex was bilaterally removed. It is easy to trace the influence

Schneider (1969) had on Mishkin et al. (1983), as both are in agreement that there are visual areas responsible for object identification and localization, and both managed to confirm the existence of two visual effects in two separate animal models. However, Mishkin et al. (1983) imply that object identification and localization are not mediated by two neighboring visual areas, and instead are the result of two separate pathways originating from the primary visual cortex that terminate either ventrally or dorsally. These two pathways would colloquially become known as the ventral 'what' pathway and the dorsal 'where' pathway. Although the evidence from both studies is compelling, one thing remained unclear: Could the ventral-dorsal pathway model be extended to humans?

From a theoretical perspective it seemed plausible as humans and monkeys are primates, and therefore the assumption that their functional and structural neuroanatomy is homologous can be made (Crick & Jones, 1993). To further complicate this matter however, it was unethical to perform any irreversible surgery on human subjects and the neuroimaging technology at the time was merely capable of static images not functional ones (Crick & Jones, 1993). The answer to this solution presented itself in the form of case studies of neurological patients. These are patients who were victims of tragic accidents and consequently sustained irreparable brain damage to a specific cortical area resulting in behavioral or cognitive deficits. Researchers began to apply the framework of ventral and dorsal pathways to neurological patients, and their findings suggested that these two pathways may potentially exist in humans (Newcombe et al., 1987). Eventually, the 'what' and 'where' visual pathways were revisited and amended to account for recent findings in human neuropsychological literature. By examining animal studies alongside human case studies, Goodale and Milner (1992) suggested that ventral and dorsal streams may be present in humans and that the distinction between these pathways is more evolved than a simple sensory distinction (i.e., ‘what’ vs ‘where’ computation). They proposed that the ventral stream is important for constructing and storing visual percepts of our surroundings, while the dorsal stream computes transformations of vision into skilled motor movements. Thus the two streams would now be differentiated in terms of output requirements, such that the ventral stream mediates ‘vision for perception’ and the dorsal stream ‘vision for action’ (Goodale & Milner, 1992). This would become known as the Goodale and Milner Perception-Action Model (PAM) and would go on to become one of the more prominent theories of visual pathways.

1.2 Visually-Guided and Memory-Guided Actions

Whether we realize it or not, as we go about our daily routines we are constantly computing and executing complex hand actions. These hand actions can be broadly categorized into two subsets of hand actions: visually-guided and memory-guided. Visually-guided, immediate actions, are those that are completed while using available visual information, such as reaching for an object while it remains in sight. Delayed, memory-guided actions are executed in the absence of visual information and are guided by previously stored visual information, such as reaching for this exact object while it is out of sight. Due to the difference in visual input required for memory and visually-guided actions, the PAM posits that visually guided and memory guided actions are controlled by different neural mechanisms (Goodale & Milner, 1992). It is believed that visually guided actions are controlled by the posterior parietal cortex of the dorsal stream, which transforms incoming visual information into a skilled motor movement (Goodale, 1998; Goodale & Humphrey, 1998). Contrastingly, memory-guided actions are handled by the inferior temporal cortex in the ventral stream which creates perceptual representations of objects, and then accesses these percepts when actions are initiated to objects that are no longer visible (Goodale, 1998; Goodale & Humphrey, 1998; Westwood & Goodale, 2003). Traditionally, tasks investigating memory-guided actions introduce a delay period prior to action onset, as this is believed to engage perceptual mechanisms within the ventral stream more so than real time visuomotor mechanisms in the dorsal stream. Delay periods usually range anywhere between a brief delay (~ 0 ms delay) up to a 3000 ms delay period (Cruikshank et al., 2014; Singhal et al., 2007; Westwood et al., 2000; Westwood et al., 2001a, 2001b; Westwood & Goodale, 2003). Correspondingly, delayed actions have been shown to be less accurate and slower overall versus immediate actions, likely because they rely more on perception-based visual information in comparison to visually-guided actions (Cruikshank et al., 2012a, 2014). Furthermore, dual-task interference has been proven to be more pronounced in delayed actions, indicating that memory and perceptual processes are possibly linked in some way and may in fact apportion similar neural real-estate (Singhal et al., 2007). Lastly, it is important to note that the presence or absence of objects to be reached to, does not correspond to a complete division of labor between the dorsal and ventral streams. For example, if you are reaching towards an object and suddenly it becomes occluded, the ventral stream does not get recruited the minute the object is out of sight (Westwood & Goodale, 2003). Instead, the ventral stream is engaged upon initial viewing of an object, storing of these object percepts and using this as template to form a perceptual motor plan for later use (Westwood & Goodale, 2003). Therefore, contingent on the availability of an object during action initiation and leading up to the action execution, the dorsal and ventral streams are fluidly deferring to one another to ensure completion of the hand action (Westwood & Goodale, 2003).

1.3 Neurological Case Studies

Case studies of neurological patients are the foundation of visuomotor theory and perhaps one of the most prominent case studies in visuomotor theory, was that of neurological patient D.F. As a result of carbon monoxide poisoning, D.F. suffered hypoxia compromising her ventral streams bilaterally, yet sparing her dorsal streams (Goodale et al., 1991; Goodale & Milner, 1992). Soon after she presented with the symptomology of visual form agnosia, and following a multitude of tests, it was established that D.F.'s perceptual impairment was solely in her visual modality and could not simply be ruled as a sensory deficit (Goodale et al., 1991). Consequently, D.F. struggles to verbally or manually communicate the shape, orientation and size of an object in front of her, yet remarkably, she is unimpaired when directing immediate actions towards this exact same object (Goodale et al., 1991; Milner et al., 2001). Interestingly, through the imposition of a two-second delay prior to action onset, D.F.'s performance deteriorates to the point that she is unable to complete the task at hand (Goodale et al., 1994). This demonstrates that the dorsal stream neural circuitry may not house visual information for long periods of time and is more suited for processing skilled and rapid visuomotor actions. Supplementary research conducted with other neurological patients possessing damaged dorsal streams but intact ventral streams, has shown that these patients are able to execute delayed but not immediate actions, suggesting that the dorsal stream may not be necessary for delayed actions (Goodale et al., 2004). Taken together, these kinematic results and neurological findings endorse the notion that perceptual judgments are mediated by ventral-stream networks, which more or less operate independently from the visuomotor dorsal stream, and that the two visual streams may function at different temporal capacities. Additionally, it seems that the ventral stream is also implicated in re-accessing previously accumulated perceptual visual information to carry out delayed actions, which are impossible for D.F. presumably due to her damaged ventral streams. This premise is supported by behavioral data collected from age- and sex-matched controls (Goodale et al., 1991, 1994; Goodale & Milner, 1992), and by additional work done involving neurologically intact populations and pictorial illusions. Specifically, healthy subjects have shown that the visual control of action is immune to these illusions but perceptual judgements are not further demonstrating a dissociation between these two kinds of visual processing. (Aglioti et al., 1995; Dewar & Carey, 2006; Haffenden & Goodale, 1998).

1.4 Area LOC

Within the ventral stream, there is one cortical region of interest with regards to delayed actions and that is the lateral occipital cortex (LOC; James et al., 2003). Anatomically, the LOC is positioned approximately in between the lateral occipital sulcus of the occipital lobe and inferior temporal sulcus of the temporal lobe (LOS; ITS; Grill-Spector et al., 2001) (Figure 1.01). The LOC was originally described in the context of object recognition and perception (Grill-Spector et al., 2001), and has been shown to be activated during initial object perception and through the endurance of the object percept (Ferber et al., 2003), and is also bilaterally damaged in patient D.F. (James et al., 2003). It is believed that the LOC processes form information in order to mediate object recognition, which could explain why D.F. struggles with not only the perception of objects but also perceptually-driven actions (Goodale et al., 1991; James et al., 2003). One fMRI study using intact populations has shown that area LOC is activated and re-activated during the action phase of delayed actions, which further suggests that this area is important for the online control of these action types (Singhal et al., 2013). Additionally, another

TMS study found that “virtual lesioning” area LOC perturbs delayed reaching but not immediate actions (Cohen et al., 2009). Although there is strong evidence in favor of area LOC subserving delayed actions, it remains unclear if this is truly the only cortical area involved in delayed reaching. Conflicting neuroimaging evidence has shown that the anterior intraparietal sulcus, a dorsal stream area, sustains activation during a delay period and virtually lesioning this area interferes with both immediate and delayed actions (aIPS; Cohen et al., 2009; Singhal et al., 2013). Other behavioral studies have also reported that the dorsal stream may be activated for delayed actions (Franz et al., 2009; Hesse & Franz, 2009). This has led to the idea that the two visual streams do not function absolutely separate from one another, and perhaps an interplay between streams is required to execute a delayed action (Cohen et al., 2009). Throughout the years in visuomotor theory, fMRI has long been a neuroimaging staple, as it offers tremendous spatial resolution which allows researchers to precisely pinpoint activated areas of interest. However, one drawback to using fMRI is that it has a very low temporal resolution, and is not able to capture the extremely rapid neural processes that occur on the order of milliseconds (Glover, 2011; Woodman, 2010). Fortunately, one alternative to fMRI is electroencephalography (EEG), as it possesses excellent temporal resolution and moderate spatial resolution. Moreover, Cruikshank et al. (2012a), have successfully demarcated an EEG signal that can be utilized to reliably quantify the differences between delayed and immediate actions. An additional benefit to using this newfound EEG signal is that it can accommodate the differences in timing needed for both immediate and delayed trials, and this in turn allows for easier identification of neural activity associated with initial activation in the ventral stream and not re-activation.

1.5 Electroencephalography (EEG)

The gyri in the human cortex contain pyramidal neurons that can produce a circular electrical field through the collective synchronized neural activity of several neurons (Binnie & Prior, 1994; Woodman, 2010). This electrical field can be detected on the scalp through electrodes, as the pyramidal neurons are naturally oriented in such a way that they are perpendicular to the electrodes (Binnie & Prior, 1994; Woodman, 2010). This is known as an EEG recording and it is not useful in its raw form, as it encompasses many neural sources of activity, making it virtually impossible to isolate any individual neural processes from one another (Luck, 2005). However, through the use of averaging and time-locking techniques on the coarse EEG recording, it is possible to extract neural responses associated with events of interest called event-related potentials (ERPs; Luck, 2005). One notable ERP component is the N170 ERP, which has been shown to have a larger amplitude under delayed reaching conditions as opposed to immediate reaching conditions (Cruikshank et al., 2012a).

1.5.1 *The N170 ERP Waveform*

Discovered in the 1990's, the N170 ERP is a negative-going peak approximately 170 ms post stimulus, generated in occipito-temporal electrode sites (Bentin et al., 1996). Conventionally, the N170 ERP has been described with regards to human facial stimuli, and is maximally and preferentially elicited during the perception of human faces among other object categories (Bentin et al., 1996; Eimer, 2012). The N170 ERP is believed to reflect structural encoding of human faces, including the extraction and subsequent configuration of internal and external human facial features (Eimer, 2000), and has been additionally shown to be modulated by human facial expressions (Blau et al., 2007). Although widely regarded as an ERP marker for face perception, it is also plausible that the N170 ERP may also be implicated in object recognition and broad perceptual processing. This is because the N170 has several neural generators, with one being the LOC (Rossion et al., 2003) which is a cortical area believed to handle these aforementioned processes (Grill-Spector et al., 2001). Since the LOC is located in the ventral stream and associated with the control of delayed actions (Cohen et al., 2009), the N170 ERP presents itself as the most appropriate candidate for studying memory-guided actions. This in fact was tested by Cruikshank et al. (2012a) who used the N170 to directly compare the neural activity of memory-guided and visually-guided actions. They hypothesized that the N170, in part, reflects activity in the ventral visual stream and thus could be used to probe activity in that stream. Therefore, memory-guided actions that depend heavily on perceptual information in the ventral stream, will elicit a larger amplitude N170, which is presumably indexing increased activity in this visual stream. Indeed, they found that the amplitude of the N170 for delayed actions was larger than immediate actions and that ERP component could be used as a robust marker for comparing these action types.

1.6 Sensorimotor Integration Signals and Reach-Height

To date, all the studies that have contributed to visuomotor theory have mainly focused on delayed and immediate actions to targets presented only in the lower visual field under the premise that this is the main visual field we operate within on a daily basis. This is surprising however, considering that many day-to-day hand actions are also initiated towards objects within the upper visual field, such as reaching for a book on a shelf. Interestingly, no one has yet compared memory- and visually-guided actions across the upper and lower visual fields using

EEG, and more specifically the N170 ERP technique. To help test this, I conducted an experiment that was partly inspired by a jump avoidance paradigm used by Bland et al. (2006). In that experiment, rats were trained to jump to different height positions to avoid being shocked while measuring the amplitude of theta, a sensorimotor signal. The main finding from that experiment, was that when rats jumped to increasing heights, such that the magnitude of the movement increases, theta amplitude is augmented (Bland et al., 2006). Interestingly, in human literature, theta signal activation is greater during the initiation and movement execution of delayed actions compared to immediate actions (Cruikshank et al., 2012b). Since there appears to be an ambiguous connection between the theta and N170 sensorimotor signals, I conducted an experiment where targets were presented at variable reach-heights as a proxy of the Bland et al. (2006) jump avoidance task, and analyzed the N170 ERP signal. At this stage, my paradigm is focused strictly on the N170 and not the theta signal. Specifically, I wanted to extend the results of Cruikshank et al. (2012a), by comparing delayed and immediate actions to targets presented across both the lower and upper visual fields, using the N170 ERP as an electrophysiological marker. As previously mentioned, memory-guided actions initiated to targets in the lower visual field are prolonged and more erroneous than visually-guided actions (Cruikshank et al., 2012a), and I predicted that this difference would be exacerbated to stimuli in the upper visual field. I tested the hypothesis that memory-guided actions to targets in the upper visual field may be more perceptually taxing, take longer to execute, and be associated with a greater amplitude N170 ERP versus visually-guided actions. If our hypothesis is confirmed, this would suggest that movement planning of delayed actions in the upper visual field reflects increased perceptual contribution from the ventral stream. In contrast, if our hypothesis is not supported this would suggest that any possible differences in perceptual demand between memory- and visually-guided actions in the upper visual field, may not be reflected in the amplitude of the N170 ERP. However, we expect to still observe some kinematic differences for these hand actions. Specifically, we expect that the movement programming involved in higher reaches should be behaviorally more effortful, and therefore delayed and immediate actions may take longer to execute or initiate to targets in the upper visual field.

Chapter 2:

Methods and Results

2.0 Methods

The methodological reporting of this thesis will be a reiteration of previously conducted and published research with minor modifications (Cruikshank et al., 2012a).

2.0.1 Participants

Twenty-eight right-handed participants (10 males, 18 females) aged from 17-34 (mean 20.4, SD = 3.8) were recruited from an undergraduate subject pool and were awarded course credit for their participation. Ten subjects were preprocessed but removed from further analyses, five of which had compromised EEG data with incessant artifactual contamination and the remaining five had both unsalvageable behavioral and EEG data. Subject inclusion for further analyses was based on the retention of at least 50% of trials per condition, following two sets of filtrations. This 50% threshold was arbitrarily set, and the ten participants previously mentioned failed to meet this criterion. All subjects provided written informed consent and were screened prior to testing for visual or auditory deficits, all of whom acknowledged they possessed intact audition and vision or corrected-to-normal vision. In accordance with standard testing procedure, all methods were approved by the Research Ethics Office at University of Alberta.

2.0.2 Procedure

The study was performed in a dimly lit Faraday chamber that has been fortified to mitigate electromagnetic and auditory interference. Inside the chamber, participants were placed in front of a 430.4 mm by 270.3 mm touchscreen oriented in the vertical direction. This was done to provide a larger range of variability along the vertical axis of interest rather than the horizontal axis. Participants were to arrange their seating position, such that they could execute hand actions adequately while maintaining a 45° reaching angle between their bicep and forearm muscles. During this preparatory phase, hand actions were examined from a side-view to ensure that the reaching distance would elicit a full 45° range of motion (i.e., subjects are not making partial reaching movements) and that there were no over compensatory biomechanical strategies (i.e., overreaching). Across the several experimental sessions, measurements of distance from the nasal electrode to the screen were recorded and fell between the following range, 48.26 cm – 60.20 cm (mean distance from the screen was 51.26 cm) (Figure 1.02). Based on average distance from the screen, the vertical and horizontal visual angles of the touchscreen were 33.78° and 46.82°, respectively. The vertical and horizontal visual angles of the stimuli were 1.98° and 1.13°, respectively. For the task, participants were expected to reach towards, and touch 9 mm x 14 mm black targets presented on a touch screen using E-Prime version 1.2 (Psychology Software Tools). Target location was drawn at random from a uniform distribution across the vertical dimension. To initiate a trial, participants depressed a button on a response box with their right index finger. Afterwards, a stimulus would appear on the screen for a variable viewing period between 1000 – 3000 ms, and participants were to direct their focus onto the black target. During this viewing period, an auditory cue of 800 Hz and 64 dB was played for 50 ms. Participants were instructed to initiate contact with the screen as precisely and swiftly as possible, but only after hearing the auditory cue. The experiment consisted of two conditions: a visually-guided condition and a memory-guided condition (Figure 1.03). In the visually-guided condition, stimulus offset was simultaneously paired with movement onset or if the subject had not engaged in movement activity for more than one second. It should be noted that visually-guided trials in the latter scenario, were all omitted from analysis. In the memory-guided condition however, stimulus offset was simultaneously paired with the sounding of the tone making it impossible to initiate the reach while the target was still on the screen. After having successfully touched the screen, participants were then to repeat the preceding instructions to initiate a new trial. That is, subjects would once again need to depress the button on the response box with their right index finger, and wait for the tone onset before initiating an action. To ensure familiarization with the paradigm, participants were provided with four practice trials with on-screen performance feedback, prior to any testing. These four practice trials were the only trials administered with assessment of performance and were later exempt from further analyses. The experiment consisted of 360 test trials in all, with 180 trials allocated to each experimental condition. Trial presentation was interleaved, such that the same condition could not be presented more than five times repetitiously. Lastly, participants were permitted a rest period every 120 trials for a preferred duration of their choosing.

2.1 Data Analysis

Following data collection, we calculated the range of pixel values across the vertical dimension, and then segmented the touch screen into four equal “bins” representing the different reach heights. Bins one to four are in order of ascending reach-height, respectively (Figure 1.04).

2.1.1 Behavioral Analyses

For all the test trials three behavioral measures were recorded for all subjects: Initiation time (IT), Movement Time (MT) and Pointing Accuracy (PA). IT was quantified as the time necessary to initiate an action when auditorily cued, while MT was the period it took to completely execute the movement following action initiation. Throughout the entirety of the experiment, target position and participant's tactile response on the touch screen were recorded. These coordinates were used to determine the distance from the center of the touch response to the center of the stimuli, which allowed us to quantify and track accuracy across trials. We classified this accuracy measurement as PA, and trials were deemed accurate if the PA between target position and touch response was 8 mm or less. Carrying forward the exclusion criteria first introduced by Cruikshank et al. (2012a), trials were removed from further analyses if ITs were ≤ 150 ms or ≥ 800 ms or MTs were ≤ 200 ms or ≥ 2000 ms. In using this behavioral criterion, overall trial retention was 96% on average following analysis using MATLAB 9.7. Initiation Time, Movement Time and Pointing Accuracy were averaged for each bin and condition and then analyzed using repeated-measures ANOVAs (SPSS Version 26.0). The ANOVA factors were reach type (visually-guided/memory-guided condition) and reach-height (bin 1/bin 2/bin 3/bin 4) and we used an alpha level of .05 for all ANOVAs performed. To mitigate violations of sphericity, Greenhouse-Geisser corrections were implemented. Lastly, we also computed Bayesian repeated-measures ANOVAs (JASP Version 0.9.0.1) using the exact same factors as the classical repeated-measures ANOVAs. We strictly reported only the Inclusion Bayes factors ($BF_{Inclusion}$) which provides a ratio of support for an effect being included versus the effect not being included and this was assessed using conventional Bayesian criteria. It should be noted that we reported the $BF_{Inclusion}$ that was computed by JASP. Namely, a $BF_{Inclusion}$ between 3 to 10 indicates some evidence, and above 10, strong evidence in favor of the inclusion of an effect. Similarly, a $BF_{Inclusion}$ between 0.1 to 0.3 provides some evidence, under and above 0.1, strong evidence against the inclusion of an effect. Lastly, a $BF_{Inclusion}$ between 0.3 to 3 provides inconclusive evidence for the inclusion of an effect.

2.1.2 EEG Recording and Analysis

Subjects were fitted with a high-density 256-channel Geodesic Sensor Net, to record the continuous EEG signal at a sampling rate of 250 Hz. One subject was sampled at 500 Hz initially, and then down sampled to 250 Hz during later preprocessing stages. Electrode impedances were kept below the 50 kΩ and the EEG signal was originally referenced to the vertex electrode (Cz) and then re-referenced to an average reference post hoc. The EEG signal was then high-pass filtered at 0.5 Hz and low-pass filtered at 30 Hz creating a filter cut-off range between 0.5 Hz and 30 Hz. Channels were rejected automatically using the "Automatic Channel Rejection" function in EEGLab, and then manually through visual inspection of the channel spectra. Independent Component Analysis (ICA) was conducted in order to distinguish and eliminate artifacts from the data. Each individual component was assessed based on topographic scalp distribution, power spectrum and single trial time course. The artifactual components detected and subsequently removed, included lateral eye movements, eye blinks and muscle artifacts which are stereotypically reported in EEG research. Following ICA preprocessing, removed channels were interpolated and the datasets were segmented into 1200-ms epochs time locked to the onset of the auditory cue (200 ms prior to the tone and 1000 ms following the tone). Epochs were then baseline corrected by subtracting the mean voltage from the 200 ms pre-stimulus activity (-200 ms to 0 ms) to mitigate variances in the ERP measurements. Lastly, ERPs were filtered on a trial-by-trial basis by applying a ±100 µV amplitude threshold and a ±25 µV slope threshold. The slope threshold accounted for physiologically implausible point-to-point differences in the ERP waveform, which allowed, for example, for the detection of large voltage spikes in the ERP waveforms. The amplitude threshold was the maximum voltage value allowed in either direction, working in tandem with the slope threshold. In utilizing a restrictive slope threshold, we became more liberal with the amplitude threshold as we felt confident that the slope threshold would filter out much of the ERP noise and the amplitude threshold would supplement the slope threshold and catch something it could not. Following voltage filtration and the preceding behavioral filtration, trials were averaged together, leaving approximately 38 trials per bin for the memory-guided condition and 36 trials per bin for the visually-guided condition.

Three ERP measures were quantified for all subjects and these included: Time-Window Mean Amplitude, Minimum Amplitude and Latency. Time-Window Mean Amplitude was the overall voltage produced by collapsing across all voltage values, while Minimum Amplitude was the average of the most negative value for the N170. Latency was specified as the time it takes for the N170 ERP to peak maximally, following the auditory cue. The N170 ERP was extracted at both 100 ms – 300 ms and 150 ms – 300 ms time windows, and the ERP measures were quantified based on these extraction windows to remain consistent with previous studies (Cruikshank et al., 2012a, 2014). Generally, the difference between the time windows did not affect the statistical outcome of our results apart from a main effect of latency in the 100 ms – 300 ms time window. We speculated that in using the more liberal time interval we may be capturing other electrophysiological sources of noise (i.e., latency jitter) that in turn are influencing the ERP waveforms. We plotted and compared the latency plots at both time windows which corroborated our suspicions and thus we proceeded with the 150 ms – 300 ms time window. ERPs were produced using EEGLab (7.1) and MATLab (9.7) and were focused mainly on individual temporal electrodes, T5 and T6. Much like with the behavioral measures, a classical repeated-measures ANOVA (SPSS Version 26.0) was used to analyze the Time-Window Mean Amplitude, Minimum Amplitude and Latency. The factors and levels of the factors were kept identical to the previous behavioral ANOVA, carrying over the same alpha level of .05 and applying Greenhouse-Geisser corrections. Once more, we computed Bayesian repeated-measures ANOVAs (JASP Version 0.9.0.1) for all the ERP measures. The factors and Bayesian criterion were retained and we only reported the $BF_{Inclusion.}$

2.2 Results

2.2.1 Behavioral Results

IT, MT, and PA were each individually collapsed across trials, at each bin and for both conditions and subsequently run through a reach type [2] (visually guided/memory-guided) X reach-height [4] (bin 1/bin 2/bin 3/bin 4) repeated-measures ANOVA. The three behavioral measures were also run through a Bayesian repeated-measures ANOVA carrying over the exact same factors and levels for each factor as the classical ANOVA. Grand-averaged IT, MT, and PA plots are shown on Figure 1.05. The descriptive statistics and classical ANOVA outputs for our behavioral analysis are reported in Tables 1.01 and 1.02, whereas the inclusion Bayes Factors for the Bayesian ANOVA are reported in Tables 1.03. On average, IT was faster for the memory-guided condition across all bins and the ANOVA showed a main effect of reach type (Figure 1.05, Table 1.02). The Bayesian ANOVA found strong evidence for the effect of reach type, $BF_{Inclusion} > 1000$ (Table 1.03). Extant literature supports these results and suggests that Initiation Time is faster for memory-guided reaching and decreases monotonically with increasing delay interval between action cueing, when compared to visually-guided reaching

(Cruikshank et al., 2012a, 2014). It is believed that this is because memory-guided actions make use of perception-based visual information, which is less accurate than real time visual information and progressively decays (Cruikshank et al., 2012a, 2014; Dijkerman et al., 1998; Goodale et al., 1994; Goodale et al., 2004; Milner & Goodale, 2006). Thus, in order to compensate for the less precise and gradually degenerating percept, participants could be initiating faster in the delayed condition (see discussion). Additionally, IT was also fastest for both conditions at the lowest bin versus the highest bin (Table 1.02), however the Bayesian ANOVA found inconclusive evidence for the effect of reach-height on IT, $BF_{Inclusion} = 0.35$ (Table 1.03). The behavioral pattern in our IT data is presumably reflecting the increase in motor planning needed for the more biomechanically demanding hand actions at the higher target positions. The MT ANOVA indicated no main effect of reach type, however there was a main effect of reach-height, showing a monotonic increase of movement time with increasing bins (Figure 1.05, Table 1.02). The Bayesian ANOVA replicated these results and found moderate evidence against the effect of condition, $BF_{Inclusion} = 0.12$, and strong evidence for the effect of reach-height, $BF_{Inclusion} > 1000$ (Table 1.03). The main effect of reach-height on MT replicates previous studies suggesting there are differences between our upper and lower visual fields, and that visuomotor performance is benefitted in the lower visual field in comparison to the upper visual field (Brown et al., 2005; Danckert & Goodale, 2001; Handy et al., 2003; Rossit et al., 2013). Lastly, the PA ANOVA failed to reveal any main effects of either reach type or reach-height (Figure 1.05, Table 1.02). Interestingly, the Bayesian ANOVA found strong evidence against the effect of reach type, $BF_{Inclusion} = 0.11$, yet strongly supported the main effect of reach-height, $BF_{Inclusion} = 13.41$ (Table 1.03). The discrepancy between the classical and Bayesian ANOVA with regards to the main effect of reach-height on PA, seems to suggest that this effect may be statistically unreliable. Nevertheless, there appears to be a non-significant trend showing an increase in PA at the higher bins (Figure 1.05). When we consider the differing monotonic patterns of MT and PA with respect to reach-height, they seem to imply some form of a speed-accuracy tradeoff. Specifically, participants appear to be taking longer to execute hand actions to targets at the higher positions, in order to preserve pointing accuracy (see discussion). All interactions between reach type and reach-height failed to reach significance for any of the behavioral measures across both the classical and Bayesian ANOVAs (Table 1.02, Table 1.03).

2.2.2 ERP Results

In accordance with our behavioral analyses, ERP measures (Time-Window Mean Amplitude, Minimum Amplitude and Latency) were averaged across all trials, at each bin for both conditions and analyzed using a reach type [2] (visually guided/memory-guided) X reach-height [4] (bin 1/bin 2/bin 3/bin 4) repeated-measures ANOVA. Additionally, a Bayesian repeated-measures ANOVA was performed for all three ERP measures, implementing the exact same factors and levels for each factor as the classical ANOVA. Grand-average ERP waveforms are shown for both temporal sites and conditions, and then binned for both conditions separately at each individual electrode in Figure 1.06. Descriptive statistics and ANOVA outputs for all ERP measures at each temporal electrode are reported in Tables 1.04 – 1.05 for T5 and Tables 1.07 – 1.08 for T6. Accordingly, the inclusion Bayes Factors for the Bayesian ANOVA are reported in Table 1.06 for T5 and Table 1.09 for T6. At the T5 temporal electrode, the ANOVA showed a main effect of reach type on both the N170 time-window mean and minimum amplitudes, as a result of the visually-guided condition having a more positive average voltage and due to the presence of more negative values in the memory-guided condition (Figure 1.06, Table 1.05). The Bayesian ANOVA found inconclusive evidence for the effect of reach type on the N170 time-window mean amplitude, $BF_{Inclusion} = 0.50$, and strong evidence for the effect of reach type on the N170 minimum amplitude, $BF_{Inclusion} = 10.15$ (Table 1.06). These results replicate those of Cruikshank et al. (2012a), who found that the difference between memory-guided and visually-guided reaching was more pronounced at the T5 temporal electrode, in comparison to the T6 temporal electrode. A main effect of reach-height was non-significant for both the N170 time-window mean and minimum amplitude ANOVAs at the T5 temporal electrode (Table 1.05). The Bayesian ANOVA supported these results and found strong evidence against the effect of reach-height on the N170 time-window mean amplitude, $BF_{Inclusion} = 0.04$, and strong evidence against the effect of reach-height on the N170 minimum amplitude, $BF_{Inclusion} = 0.03$ (Table 1.06). Although not significant, the binned figures also showed a bigger N170 difference between conditions at the T5 temporal electrode than the T6 temporal electrode, which served as a cross-check for our unbinned analysis (Figure 1.06). In addition, the N170 latency ANOVA at the T5 temporal electrode revealed no statistically significant main effects of reach type or reach-height (Table 1.05) and this was supported by the Bayesian ANOVA (Table 1.06). For the N170 time-window mean amplitude, minimum amplitude and latency ANOVAs at T5, there were no significant interactions to report (Table 1.05). Similarly, the Bayesian ANOVA found strong evidence against an interaction between reach type and reach-height for all ERP measures at T5 (Table 1.06). Lastly, all classical and Bayesian ANOVAs at the T6 temporal electrode revealed no significant effects or interactions (Table 1.08, Table 1.09).

Chapter 3:

Discussion

3.0 Discussion

Our main research objective was to use the N170 ERP to directly compare neural processes underlying delayed and immediate actions initiated to targets at different reach-heights. Compared to visually-guided actions, memory-guided actions are known to be slower and less accurate in the lower visual field because they rely heavily on perception-based information (Cruikshank et al., 2012a, 2014; Goodale et al., 1994). We expected this pattern to extend into the upper visual field, resulting in further behavioral and perceptual demand for delayed actions. Therefore, we hypothesized the N170 for memory-guided actions in the upper visual field would increase in amplitude reflecting increased perceptual processing in the ventral stream. Contrary to our hypothesis, there was not an interaction between reach-height and either reaching type suggesting that hand-arm kinematics and the neural circuitry underlying visually- and memory-guided actions may be more similar for targets in the upper visual field. In other words, perceptual demands are not increased for memory-guided actions any more than they are for visually-guided actions to targets in the upper visual field. Moreover, delayed actions initiated faster than immediate actions across all reach-heights, but the two conditions did not differ from one another in terms of accuracy or movement time. Finally, the N170 exhibited a greater amplitude difference between conditions in the left hemisphere versus the right hemisphere, which replicates previous visuomotor literature. This finding suggests that movement planning for delayed actions might be lateralized to the left-hemisphere or it may be a consequence of subjects using their right hand in this study. Our kinematic and electrophysiological results, predominantly fell within what has been formerly reported in studies investigating delayed and immediate reaching, which we discuss below.

3.1 Discussion of Behavioral Results

3.1.1 Initiation Time

As stated earlier, we discovered a main effect of trial type on IT. This finding was strongly supported by the inclusion Bayes Factor. Specifically, there is a 28 ms constant difference across conditions and all vertical bins with memory-guided reaching having an overall faster IT. This result integrates with previous findings as Cruikshank et al. (2012a) also found that delayed actions initiated faster than immediate actions and that increasing delay periods systematically decreases IT (Cruikshank et al., 2014). Together, our collective findings imply that memory-guided actions may initiate faster because they are mediated by perceptual mechanisms in the ventral visual stream. As previously mentioned, the ventral stream constructs relative representations of our environment and objects for downstream identification and perceptual processing (Dijkerman et al., 1998; Goodale et al., 2004; Milner & Goodale, 2006). These perceptual representations are presumably accessed the moment vision is occluded prior to action initiation (Westwood & Goodale, 2003), such as in our memory-guided condition. Naturally, the visual information within these percepts is believed to be less accurate than the information that is available in real time, because they are based on relational representations of objects and our environment. In addition, these perceptual representations are also known to decay, and will become progressively less accurate with time (Cruikshank et al., 2014). Therefore, participants could be initiating faster in our delayed condition, because the visual information is less precise to start with and there is an urgency to act as quickly as possible to counteract this decay. In-turn, this would ensure that the planning and execution of memory-guided actions would be slightly more accurate. By contrast, our visually-guided condition has real-time visual information available until movement initiation, allowing for more time to accurately plan and execute the movement without any decay. Therefore, participants may not feel as compelled to initiate their actions as rapidly in the immediate condition, for this exact reason. To our knowledge, only two other studies, Westwood and Goodale (2003) and Singhal et al. (2007), have investigated delayed and immediate actions in a similar manner to our study, while also measuring IT. Both studies found different results for IT than what we reported; however, it is important to consider that there are numerous differences between our study and theirs. Among other things, the fundamental difference is that both Westwood and Goodale (2003) and Singhal et al. (2007) implemented tasks focused around precision grasping of a target whereas our task involved basic pointing towards a target. Thus, it is difficult to directly compare our results with theirs because the movement planning and initiation of precision grasping is much more complex than that of simple pointing.

Nevertheless, an alternative explanation for our IT result is that it may suggest there is an attentional effect in the delayed condition. As outlined earlier in our methods section, in this condition the target is extinguished simultaneously with the sounding of the tone. This instantaneous change of the target availability when the tone is introduced, is both conspicuous and intuitive which could be capturing the attention of the participant. Thus, participants could be initiating faster in the delayed condition because the design of this trial type is unexpectedly providing some attentional advantage. By contrast, participants do not gain any additional attentional benefits in the visually-guided condition. This is because in this condition, the target disappearance is now paired with movement initiation and not with the tone. In other words, the tone will sound on and off and the stimulus will remain on the screen until the participant has initiated their action (for a maximum of 1000 ms without action initiation). Although the configuration of this trial type prevents an attentional effect, it perhaps points towards another explanation. Across both reaching conditions, participants may be learning that as long as the stimulus remains on the screen, that they should inhibit their movement. This learned association will not affect the delayed condition, because the target will disappear with the onset of the auditory cue and the participants will know to initiate a movement. However, participants will need to make an exception in the visually-guided condition. This is because only in this trial type, and only following the tone, the presence of the target no longer means "withhold movement". Therefore, participants may need to override this learned association in this condition, which is systematically lengthening the IT by 28 ms. Attentional effects and learned associations have important implications for delayed and immediate actions and our finding replicates previous work done in our lab (Cruikshank et al., 2012a).

Likewise, we also discovered a main effect of reach-height on IT. That is, both memory- and visually-guided actions are initiated 9 ms faster for the lowest bin versus the highest bin. This finding is sensible because as hand actions increase with reach-height they are becoming more effortful, with actions at the highest bin being the most biomechanically complex. Accordingly, this linear increase in complexity of the hand action likely demands an equal increase in the time needed to properly plan the movement. Presumably, it is this increase in the duration of the movement planning, that the behavioral pattern of our IT data is reflecting. However, it is important to mention that the inclusion Bayes Factor indicates that this main effect is inconclusive, and perhaps more data is required. Overall, our IT results replicate the findings of Cruikshank et al. (2012a) and Cruikshank et al. (2014) demonstrating that memory-guided actions initiate faster than visually-guided actions. However, we also extend and supplement this narrative by novelly reporting that both delayed and immediate actions initiate fastest at the lowest reach-height and slowest at the highest reach-height.

3.1.2 Movement Time

We discovered a main effect of reach-height on MT, with MT increasing by a minimum of 23 ms with increasing reach-height and that there is a 90 ms difference between the lowest and highest bins, respectively. The inclusion Bayes Factor indicates there is strong evidence for this finding. The longer movement times across the higher bins corroborates the well-recognized notion that hand actions are fastest within the lower visual field versus the upper visual field (Brown et al., 2005; Danckert & Goodale, 2001; Rossit et al., 2013). Moreover, the monotonic pattern in our MT data complements the parallel monotonic pattern of our IT data. As biomechanical effort increases for immediate and delayed actions with ascending bins, more time is needed to plan the movement thus lengthening IT. In addition to this, the movement execution of these hand actions is similarly taking longer as there is a greater biomechanical demand for the higher target positions. Surprisingly, unlike Cruikshank et al. (2012a), a main effect of condition was not found. Based on the inclusion Bayes Factor, there is moderate evidence against this effect as well. An interpretation of this result follows. It is possible that the higher reaches are equally more difficult for both memory-guided and visually-guided actions, which is why MT was becoming similarly slower for both of these hand actions. Accordingly, MT differences between trial types could be more subtle and harder to detect in our experiment compared to Cruikshank et al. (2012a). Therefore, the lack of a main effect of condition on MT could be because the main effect of reach-height is washing out and superseding any possible differences between conditions. Outside of the work done by our lab group, our result also deviates from previous studies that found that actions to remembered targets have slower movement times than actions to targets in real time (Armstrong & Singhal, 2011; Goodale et al., 1994; Singhal et al., 2007; Westwood et al., 2000; Westwood et al., 2001a, 2001b). It is important to consider, however, that most of the extant literature surrounding the longer MT of memory-guided actions revolves around hand actions or tasks that are crucially different and much more complex than what we are studying. In particular, most visuomotor studies typically implement an occlusion event which extinguishes the entire field of view in addition to requiring participants to perform a precise grasping action (Goodale et al., 1994; Milner et al., 2001; Singhal et al., 2007; Westwood et al., 2000; Westwood et al., 2001b). Therefore, the novelty of our MT finding may not actually contradict any published research but is perhaps attributable to differing experimental paradigms and objectives than past studies.

3.1.3 Pointing Accuracy

Lastly, we did not reveal a main effect of condition for PA and did not replicate the results of Cruikshank et al. (2012a). Correspondingly, the absence of a main effect of trial type on PA was moderately supported by the Bayesian ANOVA. Furthermore, the main effect of reach-height also failed to reach significance for PA. Surprisingly, the inclusion Bayes Factor indicates strong evidence for this finding. Although the Bayesian ANOVA strongly supported the main effect of reach-height, the classical ANOVA found the main effect of reach-height was non-significant with a relatively low p-value (p = .14) thus they are not technically in contradiction with one another. The null effect of reach-height in the classical ANOVA we suspect should be viewed more like a "true null". At the same time, the large inclusion Bayes Factor for that effect, suggests that we should not draw such a conclusion so quickly. For this reason, we consider it unresolved whether the main effect of reach-height on PA is present or not. Moreover, there appears to be a non-significant trend in our PA data showing that both memory- and visually-guided actions are equivalently becoming more accurate with the higher bins. The behavioral pattern in our PA data may not make sense alone but becomes easier to understand when analyzed alongside the MT data. The monotonic patterns in both the PA and MT data are completely inverse to one another. Interpreted jointly, they demonstrate a speed–accuracy trade off function. Participants appear to be sacrificing their movement speed to achieve greater accuracy at the higher bins. Although there were no significant findings for PA, the behavioral pattern in the PA data supports those of IT and MT and there appears to be continuity among all behavioral measures. Particularly, both memory- and visually-guided actions take longer to initiate and execute in order to preserve accuracy with increasingly higher and more biomechanically complex reaches.

3.2 Discussion of ERP Results

3.2.1 Un-binned ERPs

The first phase of our N170 ERP analyses revolved around checking for a replication with Cruikshank et al. (2012a). However, their task did not involve a reach-height element and they were strictly measuring differences between conditions at temporal electrodes T5 and T6. Therefore, to remain consistent when comparing our ERP results with theirs, we averaged our N170 waveforms across all bins and compared trial type differences at both temporal electrodes. At T5 we revealed a main effect of trial type on the N170 minimum amplitude. This main effect was also strongly supported by the Bayesian ANOVA. The minimum amplitude was calculated by locating the most negative voltage in the 150 ms – 300 ms time window and averaging all those voltage values collectively for all trials, subjects and both conditions. Since there are no other components that peak negatively within the specified time window, we believe this negative value to be a good estimate of the amplitude of the N170. Our result indicates that on average, the N170 for the delayed condition is more negative compared to the immediate condition and there was a -1.00 µV amplitude difference between conditions. This finding again fits with the results of Cruikshank et al. (2012a) who also found an amplitude difference between trial types at T5, with memory-guided actions eliciting a more negative N170 ERP. As previously mentioned, memory-guided actions likely rely on some perception-based visual information to a greater degree than visually-guided actions. Thus, the increased negativity in the N170 amplitude in the delayed condition is likely reflecting increased activation of perceptual mechanisms within the ventral visual stream. In other words, the enhancement of the N170 amplitude for memory-guided actions further demonstrates that these hand actions may be more perceptually demanding than their visually-guided counterparts. The strong consistency of our ERP result with Cruikshank et al. (2012a), provides further evidence that the N170 is a reliable electrophysiological marker for indexing perceptual processing in the ventral stream. We also discovered a main effect of condition on the time-window mean amplitude of the N170. Namely, the time-window mean amplitude of the N170 is +0.63 µV more positive in the visually-guided condition than for the memory-guided condition. This result makes sense given the voltage values across the time window for both conditions. In the visually-guided trials there are positive voltage values before and after the N170, and the N170 itself is also less negative on average. Conversely, the reverse is true for the memory-guided trials, as the voltage values prior to and following the N170 are more negative-going and the N170 is more negative on average. Accordingly, this underlying difference between trial types is going to carry over into the mean amplitude calculation. The time-window mean amplitude is determined by averaging together all the voltage values across the entirety of the 150 ms – 300 ms time window for all trials, subjects and for both conditions. Simply stated, the amplitude of the N170 along with all the voltage values preceding and subsequent to this peak are averaged together as they both fall within the specified time window. Since the immediate condition has more positive voltage values across the time window, naturally the mean amplitude is going to be more positive and larger. By the same token, there are more negative values in the delayed condition, which is the reason the mean amplitude for the entire time window is smaller and less positive. Thus, the main effect of trial type on the time-window mean amplitude supplements the earlier cited main effect of condition on the minimum amplitude. Finally, the inclusion Bayes Factor suggests there is inconclusive evidence for the main effect of condition on the time-window mean amplitude and thus more data should be collected.

However, at T6 our ERP findings seem to diverge from Cruikshank et al. (2012a). In their ERP analyses, they discovered amplitude differences between conditions at both T5 and T6, although the difference was larger at T5. However, we revealed no main effects and no trial type differences at T6. There is strong support for the lack of main effects at T6, based on the inclusion Bayes Factors. One interpretation for this result is that it can be explained by how the motor and visual areas interact within each cerebral hemisphere. The motor areas in each hemisphere are cross-wired, which means that the left hemisphere motor areas control the right half of the body (i.e., right-handed actions), while the right hemisphere motor areas control the left half of the body (i.e., left-handed actions). Moreover, these motor areas act on information from visual areas within the same hemisphere with no crossing over required. In other words, left-sided visual areas are connected more directly to left-sided motor areas, and the opposite is true for right-sided visual and motor areas. Presumably, the left ventral stream is more important for right-handed actions and the right ventral stream for left-handed actions. Since T5 and T6 are thought to overlie the left and right ventral streams, it is understandable that we found no trial type differences at T6. For our experiment, all the participants that were recruited were right-handed and only used their dominant hand throughout the task. Therefore, the right-sided motor areas in the right hemisphere will not necessarily be relevant to our paradigm, and accordingly neither will the right ventral visual stream. It is worth noting that the lack of trial-type differences at T6, cannot be explained by differences in visual information going to each hemisphere. The only thing we manipulated was the target location, but we did not manipulate how this information is represented in the visual fields as we instructed participants to fixate on the target. Therefore, we can assume that the location of the target is equally represented in both visual fields and that the visual information is transmitted symmetrically to both hemispheres. Taken together, the findings at T5 and T6 indicate that there are hemispheric differences in right-handed populations, such that the left hemisphere is more involved in planning of delayed actions than the right hemisphere.

Previous work examining the nature of hemispheric specialization for action, by Gonzales et al. (2006), has shown that the left hemisphere may be specialized for the visual control of action. In their experiment, left- and right-handed subjects were instructed to precisely grasp an object implanted within a visual illusion using both their dominant and non-dominant hands. Previous studies using pictorial illusions have shown robust effects on perception but not visually-guided grasping, but these studies only examined right-handed participants (Aglioti et al., 1995; Dewar & Carey, 2006; Haffenden & Goodale, 1998). However, the Gonzalez et al. (2006) study found that left-handed actions in both groups were not immune to the illusions, but that right-handed actions were immune. The main interpretation from this study is that independent of handedness, the left-hemisphere may be specialized for the mediation of visuomotor actions (Gonzalez et al., 2006). It is believed that this is because there is a greater functional distinction between the ventral and dorsal streams in the left-hemisphere (Radoeva et al., 2005), and thus the dorsal stream may be dominant in this hemisphere. Finding an effect at T5 but not T6, seems to align with the theory of hemispheric specialization posited by Gonzalez et al. (2006). However, our results are not fully in line with theirs, because we revealed a main effect of memory-guided actions but not visually-guided actions. Indeed, our findings indicate that the left hemisphere may also be specialized for movement programming of delayed actions and seemingly contradicts the primary conclusion of Gonzalez et al. (2006). There are many reasons why our results do not fully correspond with theirs and they are outlined as follows. Firstly, because Gonzalez at al. (2006) were strictly investigating dorsal stream mechanisms in the left hemisphere, their entire paradigm revolved around visually-guided trials. Conversely, our task was probing ventral stream processes utilizing an established perceptual marker (i.e., the N170) and involved both delayed and immediate reaching conditions across variable heights to be reached to. Put another way, both our research objectives and experimental designs are fundamentally different from the outset. Secondly, in their study participants were instructed to accurately grasp objects embedded within visual illusions, when by comparison our subjects initiated pointing actions to uniform targets. Grasping is a considerably more complex action because it involves calculating the dimensions of the target object, the distance between the thumb and index finger and location of the object in space. By contrast, pointing actions simply requires spatial localization of the hand towards a target object. Thirdly, Gonzalez et al. (2006) are presumably manipulating perceptual contribution by utilizing pictorial illusions, whereas we are doing so through the insertion of a delay in our delayed reaching condition. It is unclear if and how memory-guided actions and visual illusions are qualitatively similar with regards to assessing perceptual mechanisms. Provided all the dissimilarities described, our results may not actually challenge the results of Gonzalez et al. (2006) but could be because a great deal of work remains to be done. It should also be noted that our results only reveal part of the story being that we only recruited a right-handed population for our paradigm. Perhaps we only revealed an effect of delayed actions at T5 because all subjects used their right hand throughout the entirety of the task and not because of a left hemisphere specialization. Ultimately, our ERP results replicate previous work conducted within our lab group (Cruikshank et al., 2012a). In a similar vein, our findings also supplement those of Gonzalez et al. (2006) in an original way, indicating that left hemisphere may potentially be specialized for both visually- and memory-guided actions.

3.2.2 Binned ERPs

The second stage of our ERP analyses involved examining the N170 at all four respective bins. This entailed averaging the N170 ERPs at every single bin for both trial types and temporal electrodes. Starting with T5, the main effects of reach-height on the time-window mean amplitude and minimum amplitude of the N170 both failed to reach significance. The absence of these main effects of reach-height were corroborated by the Bayesian ANOVA, which found strong evidence against these findings. In the immediate reaching condition, all the waveforms seem to be clustered together near the baseline, apart from the N170 ERP at bin 4 which is shifting upwards from the baseline. This non-significant trend likely has a simple explanation. For all bins in the visually-guided condition, there is a positive peak introduced around the 150 ms mark that is overlapping with the N170. This ‘P150’ seems to be slightly increasing in positivity across all the bins, with the most positive peak being in bin 4. Moreover, this positive source also appears to be lasting longer than the actual N170 itself across all the bins. When generating an ERP waveform, the voltage values are calculated across the entirety of the time-window that is defined. This means that for all reach-heights, this ‘P150’ peak will get added to the N170 and so on, resulting in a waveform that reflects the sum of all voltage values for the whole time-window. Naturally, the N170 ERPS for bins 1 – 3 will all travel towards the baseline with the N170 for bin 4 exceeding the baseline considering it has the most positive-going peak across all the bins. Therefore, the N170 ERPs in the visually-guided trial may not represent differences in reach-height but could be because this ‘P150’ is persisting and skewing the voltage values in a more positive direction.

For the delayed condition however, the waveforms appear to be demonstrating a different trend altogether. Interestingly, the N170 ERPs are simultaneously peaking and are closer to baseline at bins 2 and 3, while those at bins 1 and 4 are also peaking together and are more negative. The morphological pattern of the memory-guided waveforms, lends support to the notion that the ventral stream may dedicate more resources to processing centralized visual information than to peripheral visual information (Brown et al., 2005). This is because targets presented in bins 2 and 3 are directly in the middle of the screen, while targets presented at bin 1 and bin 4 are more peripherally located near the top and bottom border of the screen. It is also worth mentioning that participants are centered relative to the screen position and thus the middle of the screen is also parallel to the eye level of the participant. Therefore, targets are going to fall more naturally on the fovea at bins 2 and 3 compared to bins 1 and 4. There are further traces of evidence aligned with this idea when comparing the binned ERP figures across conditions. In doing so, it is clear that the difference between memory- and visually-guided reaching is the most prominent at bin 1 and bin 4 and the least prominent at bins 2 and 3. In a general sense, the pattern of the binned ERPs in the delayed condition deviates from our main hypothesis. This is because we predicted memory-guided actions in the upper visual field would be the most perceptually taxing and this would be reflected in the amplitude of the N170. In our experiment, the lower and upper visual fields are seemingly represented by bins 1 and 4. Reaching towards peripherally presented targets that fall within these bins, is accordingly presumed to reflect hand actions performed in differing visual fields. The non-significant trend in the memory-guided N170 ERPs seems to suggest that delayed actions in the upper and lower visual fields may tax perceptual processes to a similar degree. Consequently, the transformation from vision to action is perhaps more complex in perceptually driven actions than previously thought. Regardless, further testing is required. At T6, there are no discernable patterns for either reaching condition across any of the bins. Once again, the Bayesian ANOVA provided strong evidence against the main effects of reach-height on the time-window mean amplitude and minimum amplitude of the N170 at T6. Furthermore, examining the ERPs across conditions reveals no differences and that the morphological patterns look almost identical to one another. These findings are consistent with the idea that there are no trial type differences in the right hemisphere, presumably because right visual and motor areas are not engaged in our task.

3.3 Conclusion

The primary goal of this experiment was to investigate and compare the neural mechanisms of delayed and immediate pointing actions initiated at variable reach-heights. Our chief hypothesis was that delayed actions to targets in the upper visual field will be more perceptually demanding than immediate actions. Our behavioral data suggests that memory-guided actions initiate faster than visually-guided actions at all reach-heights, but both trial types are identical in terms of movement time and accuracy. Furthermore, our ERP data replicated the findings of Cruikshank et al. (2012a; 2014) and we found a larger, left hemispherical difference in the N170 amplitude between reaching conditions. However, reach-height did not differentially influence either one of the reaching conditions in a significant manner. This suggests that neural processes underlying immediate and delayed actions are more similar in the upper visual field than once thought. One potential limitation of our study is that we did not incorporate fixation crosses when comparing hand actions across the lower and upper visual fields. This is conventionally done so that targets can be presented across the visual fields, while strictly controlling participant eye and head movements. Instead, we manipulated stimulus location in our task, telling participants to fixate on the target and allowing free-viewing. This means that participants could freely shift their eye movements, and potentially their head movements, anywhere on the screen. Admittedly, we cannot be certain that target presentation was fully uniform across both the upper and lower visual fields. Future directions in electrophysiological research should explore the potential use and impact of fixation crosses on delayed and immediate pointing actions in the lower and upper visual fields. In short, this study is the first of its kind to apply the ERP technique and directly compare the neural bases of visually- and memory-guided actions across the upper and lower visual fields. Our experimental findings support a large volume of neuropsychological and neuroimaging work and previous work done in our lab. This further substantiates the notion that the N170 ERP reflects increased ventral stream activation during delayed actions. Moreover, our results provide additional evidence that the left hemisphere may be specialized for the movement programming of both memory- and visually-guided actions.

Figure 1.01

Figure 1.01 Caption:

Anatomical Position of Lateral Occipital Cortex (LOC). The LOC is located beneath the Lateral Occipital Sulcus (LOS) and near the posterior portion of the Inferior Temporal Sulcus (ITS). Please note, the anatomical positions of all the cortical regions listed above, are all approximate locations based on extant literature. Adapted and modified from Grill-Spector et al. (2001).

Figure 1.02

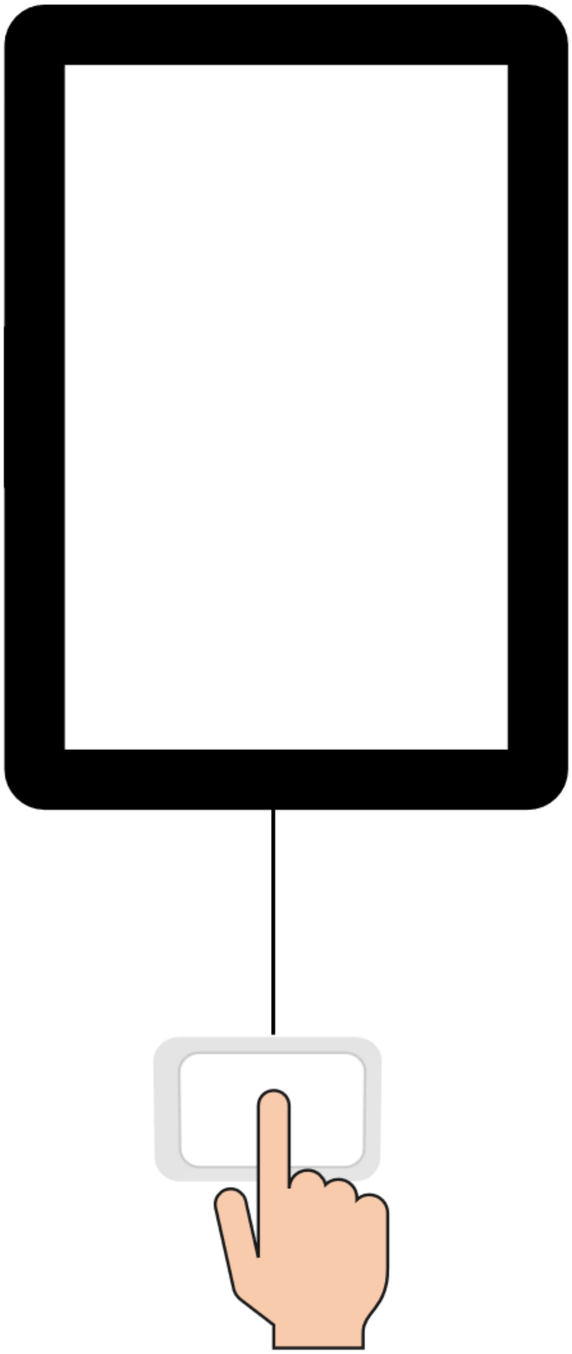

Figure 1.02 Caption:

Visualization of the experimental set-up, as shown from the frontal view of a participant. Participants were positioned in front of the touch screen and were instructed to depress a button on a response box in front of them with their right index finger. The participants hand, head, body positions and the response box position were all centralized relative to the screen. The touch screen height was adjusted to ensure that the eyeline of the participant was parallel to the center of the screen. Lastly, distance from the screen was adjusted accordingly per participant and hand actions were examined from a side-view to ensure that the reaching distance would elicit a full 45° range of motion and that there were no over compensatory biomechanical strategies. The mean distance from the screen across all subjects was 51.26 cm.

Figure 1.03

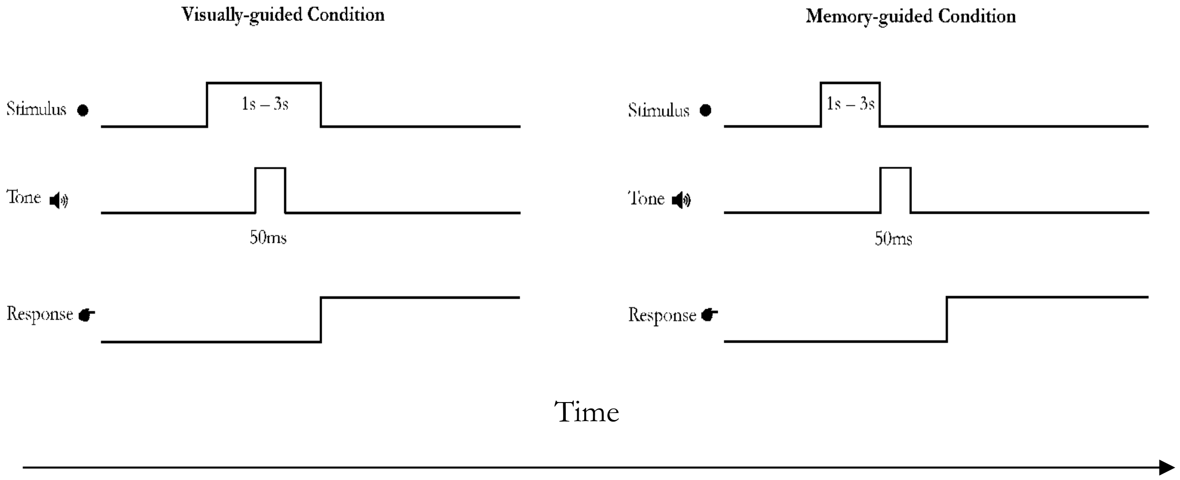
Visually-guided Condition
Memory-guided Condition
Stimulus
1s – 3s
Tone
50ms
Response
Stimulus
1s – 3s
Tone
50ms
Response
Time

Figure 1.03 Caption:

Schematic of the two experimental conditions administered throughout the experiment. In the visually-guided condition, stimulus offset is simultaneous with movement onset. In the memory-guided condition stimulus offset is simultaneous with tone onset. There were 180 trials administered per condition for one experimental session. Adapted from Cruikshank et al. (2012a).

Figure 1.04

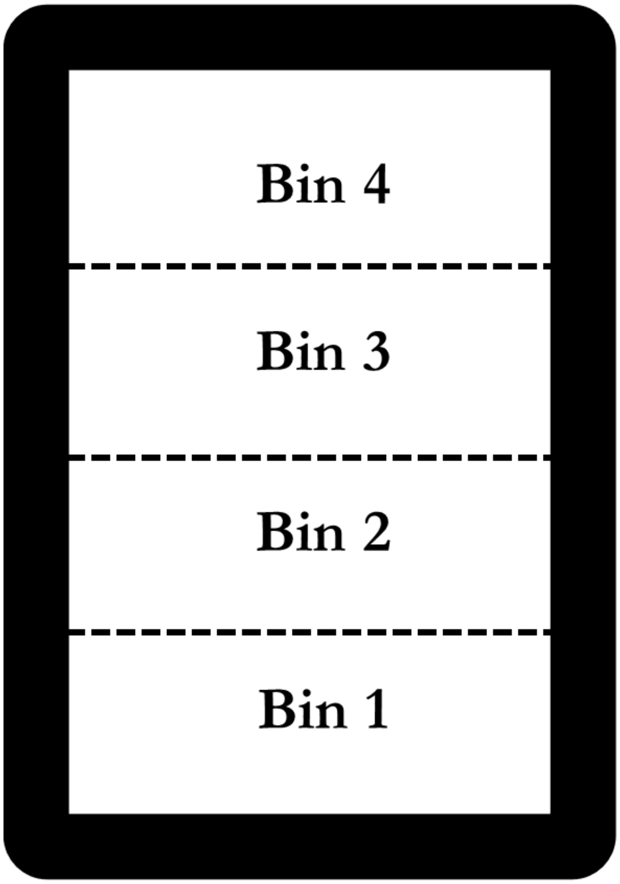

Figure 1.04 Caption:

Frontal view of the screen, which was segmented into four bins following data collection. Subjects were naïve as to which bin they were reaching to and were only instructed to reach towards a target that could appear anywhere in the screen. Location and presentation of stimulus were uniformly distributed throughout all experimental trials. Bins represent reach-height in ascending order, with bins one and four serving as the lowest and highest reach-heights respectively.

Figure 1.05

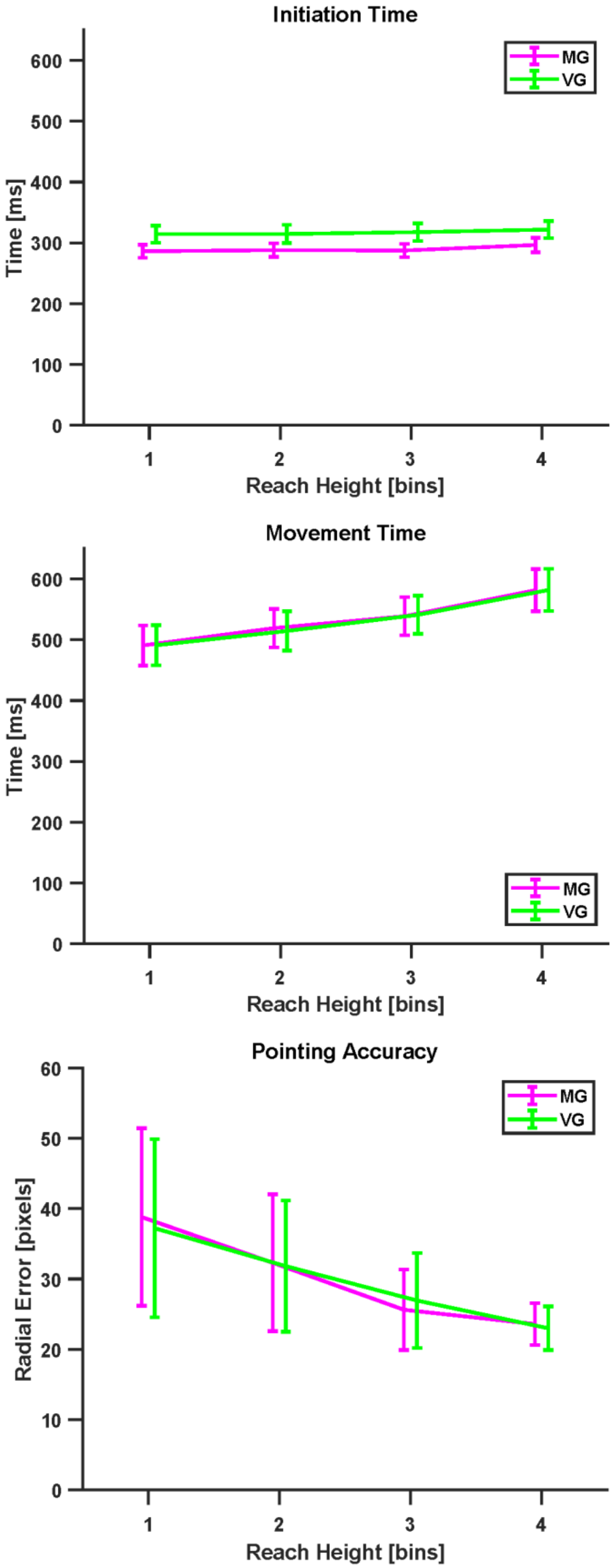
Initiation Time
Time [ms]
0
100
200
300
400
500
600
1
2
3
4
Reach Height [bins]
MG
VG
Movement Time
Time [ms]
0
100
200
300
400
500
600
1
2
3
4
Reach Height [bins]
MG
VG
Pointing Accuracy
Radial Error [pixels]
0
10
20
30
40
50
60
1
2
3
4
Reach Height [bins]
MG
VG

***Figure 1.05 Caption*:**

Top Panel: Initiation Time grand average plotted for the memory-guided (MG) and visually-guided (VG) test conditions. Reach-height (bins 1 – 4) is plotted on the x-axis and time (ms) is plotted on the y-axis. Error bars represent SEM. MG and VG are jittered horizontally by ±0.05 to facilitate visualization of error bars.

Middle Panel: Movement Time grand average plotted for the memory-guided (MG) and visually-guided (VG) test conditions. Reach-height (bins 1 – 4) is plotted on the x-axis and time (ms) is plotted on the y-axis. Error bars represent SEM. MG and VG are jittered horizontally by ±0.05 to facilitate visualization of error bars.

Bottom Panel: Pointing Accuracy grand average plotted for the memory-guided (MG) and visually-guided (VG) test conditions. Reach-height (bins 1 – 4) is plotted on the x-axis and radial error (pixels) is plotted on the y-axis. Error bars represent SEM. MG and VG are jittered horizontally by ±0.05 to facilitate visualization of error bars.

Figure 1.06

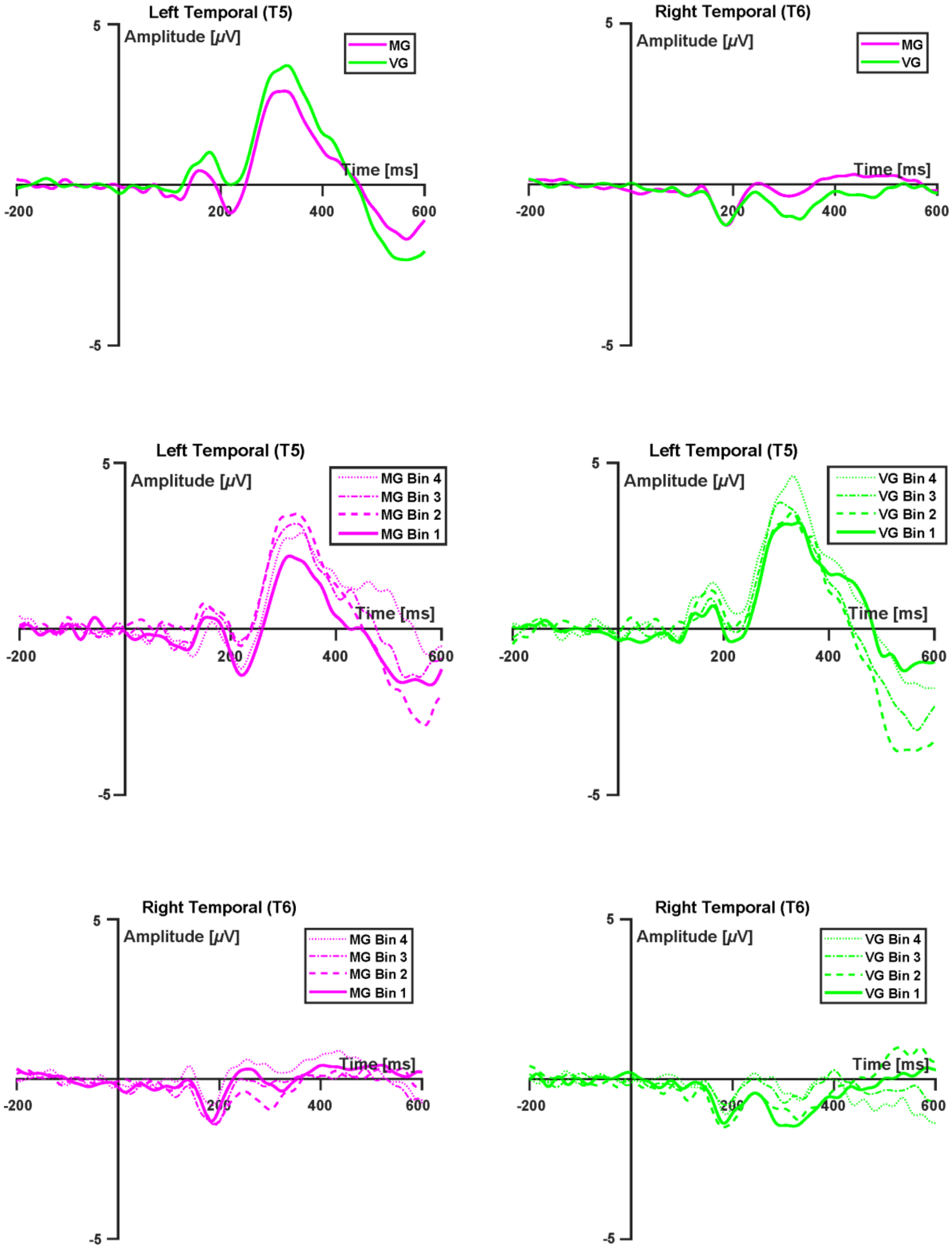
Left Temporal (T5)
Amplitude [μV]
MG
VG
Time [ms]
5
-5
-200
200
400
600
Right Temporal (T6)
Amplitude [μV]
MG
VG
Time [ms]
5
-5
-200
200
400
600
Left Temporal (T5)
Amplitude [μV]
MG Bin 4
MG Bin 3
MG Bin 2
MG Bin 1
Time [ms]
5
-5
-200
200
400
600
Left Temporal (T5)
Amplitude [μV]
VG Bin 4
VG Bin 3
VG Bin 2
VG Bin 1
Time [ms]
5
-5
-200
200
400
600
Right Temporal (T6)
Amplitude [μV]
MG Bin 4
MG Bin 3
MG Bin 2
MG Bin 1
Time [ms]
5
-5
-200
200
400
600
Right Temporal (T6)
Amplitude [μV]
VG Bin 4
VG Bin 3
VG Bin 2
VG Bin 1
Time [ms]
5
-5
-200
200
400
600

Figure 1.06 Caption:

Top Two Panels: N170 ERP waveforms grand averaged for the memory-guided (MG) and visually-guided (VG) test conditions at contralateral and ipsilateral temporal electrodes, T5 and T6. Time (ms) is plotted on the x-axis and amplitude (μV) is plotted on the y-axis.

Middle Two Panels: N170 ERP waveforms grand averaged and binned for the memory-guided (MG) and visually-guided (VG) test conditions only at contralateral temporal electrode, T5. Time (ms) is plotted on the x-axis and amplitude (μV) is plotted on the y-axis.

Bottom Two Panels: N170 ERP waveforms grand averaged and binned vertically for the memory-guided (MG) and visually-guided (VG) test conditions only at ipsilateral temporal electrode, T6. Time (ms) is plotted on the x-axis and amplitude (μV) is plotted on the y-axis.

Table 1.01

Mean Initiation Time, Movement time and Pointing Accuracy (with Standard Deviations)

Initiation Time (ms)

	VG	MG	Marginal Mean
Bin 1	314.25 ± 73.87	286.07 ± 56.93	300.16
Bin 2	314.53 ± 80.15	287.87 ± 59.07	301.20
Bin 3	317.56 ± 77.12	287.36 ± 57.60	302.46
Bin 4	321.76 ± 74.48	296.44 ± 62.57	309.10
Marginal Mean	317.02	289.44	

Movement Time (ms)

	VG	MG	Marginal Mean
Bin 1	490.98 ± 174.57	490.72 ± 174.58	490.85
Bin 2	514.47 ± 172.05	519.14 ± 167.96	516.80
Bin 3	541.01 ± 166.68	538.74 ± 166.91	539.88
Bin 4	581.90 ± 183.40	581. 48 ± 184.15	581.69
Marginal Mean	532.09	532.52	

Pointing Accuracy (pixels)

	VG	MG	Marginal Mean
Bin 1	37.22 ± 67.14	38.81 ± 66.81	38.02
Bin 2	31.82 ± 49.47	32.31 ± 51.54	32.06
Bin 3	26.93 ± 35.75	25.62 ± 30.31	26.27
Bin 4	22.98 ± 16.50	23.59 ± 15.70	23.29
Marginal Mean	29.74	30.08	

Table 1.02

Classical ANOVA Outputs for Behavioral Measures

Initiation Time

	df	Error df	F	*p*	η_p^2
Reach Type	1.00	27.00	31.41	< .001	.54
Reach-Height	2.41	65.13	5.98	.002	.18
Reach Type x Reach-Height	1.96	52.93	0.26	.77	.01

Movement Time

	df	Error df	F	*p*	η_p^2
Reach Type	1.00	27.00	0.04	.85	.001
Reach-Height	1.83	49.42	109.93	< .001	.80
Reach Type x Reach-Height	2.88	77.79	0.76	.51	.03

Pointing Accuracy

	df	Error df	F	*p*	η_p^2
Reach Type	1.00	27.00	0.57	.46	.02
Reach-Height	1.01	27.34	2.40	.14	.08
Reach Type x Reach-Height	2.57	69.34	1.50	.23	.05

Table 1.03

Analysis of Effects for Behavioral Measures

Initiation Time

Effects	P(incl)	P(incl|data)	$BF_{Inclusion}$
Reach Type	0.60	1.00	>1000
Reach-Height	0.60	0.35	0.35
Reach Type x Reach-Height	0.20	0.02	0.08

Movement Time

Effects	P(incl)	P(incl|data)	$BF_{Inclusion}$
Reach Type	0.60	0.15	0.12
Reach-Height	0.60	1.00	>1000
Reach Type x Reach-Height	0.20	0.008	0.03

Pointing Accuracy

Effects	P(incl)	P(incl|data)	$BF_{Inclusion}$
Reach Type	0.60	0.14	0.11
Reach-Height	0.60	0.95	13.41
Reach Type x Reach-Height	0.20	0.006	0.02

Table 1.04

Time-Window Mean Amplitudes, Minimum Amplitudes and Latencies (with Standard Deviations) for the N170 ERP at T5 (Left Temporal)

Time-Window Mean Amplitude (µV)

	VG	MG	Marginal Mean
Bin 1	0.64 ± 4.31	-0.09 ± 3.35	0.27
Bin 2	1.00 ± 5.87	0.80 ± 5.50	0.90
Bin 3	0.95 ± 5.75	0.70 ± 6.66	0.82
Bin 4	1.41 ± 7.66	0.07 ± 6.33	0.74
Marginal Mean	1.00	0.37	

Minimum Amplitude (µV)

	VG	MG	Marginal Mean
Bin 1	-1.59 ± 4.57	-2.87 ± 4.33	-2.23
Bin 2	-1.35 ± 5.92	-2.09 ± 5.78	-1.72
Bin 3	-1.65 ± 5.82	-2.12 ± 7.45	-1.89
Bin 4	-1.10 ± 8.23	-2.92 ± 7.05	-2.01
Marginal Mean	-1.42	-2.50	

Latency (ms)

	VG	MG	Marginal Mean
Bin 1	202.29 ± 33.73	211.57 ± 39.01	206.93
Bin 2	209.29 ± 40.50	208.86 ± 35.26	209.07
Bin 3	208.29 ± 38.16	208.14 ± 34.50	208.21
Bin 4	212.57 ± 46.10	206.14 ± 35.47	209.36
Marginal Mean	208.11	208.68	

Table 1.05

Classical ANOVA Outputs for the N170 ERP Measures at T5 (Left Temporal)

Time-Window Mean Amplitude

	df	Error df	F	*p*	η_p^2
Reach Type	1.00	27.00	5.67	.03	.17
Reach-Height	1.67	44.71	0.39	.64	.01
Reach Type x Reach-Height	2.72	73.42	1.81	.16	.06

Minimum Amplitude

	df	Error df	F	*p*	η_p^2
Reach Type	1.00	27.00	19.77	< .001	.42
Reach Height	1.60	43.02	0.23	.75	.008
Reach Type x Reach-Height	2.49	67.14	1.89	.15	.07

Latency

	df	Error df	F	*p*	η_p^2
Reach Type	1.00	27.00	0.02	.88	.001
Reach-Height	2.49	67.20	0.09	.95	.003
Reach Type x Reach-Height	2.75	74.18	0.64	.58	.02

Table 1.06

Analysis of Effects for the N170 ERP Measures at T5 (Left Temporal)

Time-Window Mean Amplitude

Effects	P(incl)	P(incl|data)	$BF_{Inclusion}$
Reach Type	0.60	0.43	0.50
Reach-Height	0.60	0.05	0.04
Reach Type x Reach-Height	0.20	0.002	0.008

Minimum Amplitude

Effects	P(incl)	P(incl|data)	$BF_{Inclusion}$
Reach Type	0.60	0.94	10.15
Reach-Height	0.60	0.04	0.03
Reach Type x Reach-Height	0.20	0.004	0.02

Latency

Effects	P(incl)	P(incl|data)	$BF_{Inclusion}$
Reach Type	0.60	0.13	0.10
Reach-Height	0.60	0.02	0.07
Reach Type x Reach-Height	0.20	3.08e -4	0.001

Table 1.07

Time-Window Mean Amplitudes, Minimum Amplitudes and Latencies (with Standard Deviations) for the N170 ERP at T6 (Right Temporal)

Time-Window Mean Amplitude (µV)

	VG	MG	Marginal Mean
Bin 1	-0.89 ± 2.60	-0.31 ± 2.86	-0.60
Bin 2	-0.91 ± 3.54	-0.78 ± 3.83	-0.85
Bin 3	-0.35 ± 4.79	-0.59 ± 4.22	-0.47
Bin 4	-0.30 ± 5.17	0.06 ± 4.41	-0.12
Marginal Mean	-0.61	-0.41	

Minimum Amplitude (µV)

	VG	MG	Marginal Mean
Bin 1	-3.13 ± 3.63	-2.57 ± 3.67	-2.85
Bin 2	-3.15 ± 4.88	-3.23 ± 5.44	-3.19
Bin 3	-2.83 ± 5.80	-2.85 ± 5.18	-2.84
Bin 4	-2.88 ± 5.98	-2.34 ± 5.22	-2.61
Marginal Mean	-3.00	-2.75	

Latency (ms)

	VG	MG	Marginal Mean
Bin 1	237.57 ± 52.40	218.57 ± 48.70	228.07
Bin 2	216.29 ± 51.36	234.00 ± 50.47	225.14
Bin 3	219.00 ± 54.95	214.29 ± 52.07	216.64
Bin 4	225.14 ± 52.99	217.14 ± 48.70	221.14
Marginal Mean	224.50	221.00	

Table 1.08

Classical ANOVA Outputs for the N170 ERP Measures at T6 (Right Temporal)

Time-Window Mean Amplitude

	df	Error df	F	*p*	η_p^2
Reach Type	1.00	27.00	2.40	.35	.03
Reach-Height	2.21	59.73	0.99	.39	.04
Reach Type x Reach-Height	2.43	65.67	1.09	.35	.04

Minimum Amplitude

	df	Error df	F	*p*	η_p^2
Reach Type	1.00	27.00	0.81	.38	.03
Reach-Height	2.45	66.14	0.48	.66	.02
Reach Type x Reach-Height	2.46	66.34	0.95	.41	.03

Latency

	df	Error df	F	*p*	η_p^2
Reach Type	1.00	27.00	0.37	.55	.01
Reach-Height	2.43	65.50	1.02	.38	.04
Reach Type x Reach-Height	2.79	75.21	2.60	.06	.09

Table 1.09

Analysis of Effects for the N170 ERP Measures at T6 (Right Temporal)

Time-Window Mean Amplitude

Effects	P(incl)	P(incl|data)	$BF_{Inclusion}$
Reach Type	0.60	0.17	0.14
Reach-Height	0.60	0.14	0.11
Reach Type x Reach-Height	0.20	0.002	0.008

Minimum Amplitude

Effects	P(incl)	P(incl|data)	$BF_{Inclusion}$
Reach Type	0.60	0.18	0.14
Reach-Height	0.60	0.05	0.04
Reach Type x Reach-Height	0.20	7.15e -4	0.003

Latency

Effects	P(incl)	P(incl|data)	$BF_{Inclusion}$
Reach Type	0.60	0.17	0.14
Reach-Height	0.60	0.07	0.05
Reach Type x Reach-Height	0.20	0.007	0.03

Bibliography

Aglioti, S., DeSouza, J. F. X., & Goodale, M. A. (1995). Size-contrast illusions deceive the eye but not the hand. *Current Biology*, *5*(6), 679–685. https://doi.org/10.1016/S0960-9822(95)00133-3

Armstrong, G. A. B., & Singhal, A. (2011). Neural markers of automatic and controlled attention during immediate and delayed action. *Experimental Brain Research*, *213*(1), 35–48. https://doi.org/10.1007/s00221-011-2774-0

Atkin, A., & Singhal, A. (2020). *Effector selection as a parallel, competitive process: Evidence from a free-choice reaching task.* Manuscript in Preperation.

Bentin, S., Allison, T., Puce, A., Perez, E., & McCarthy, G. (1996). Electrophysiological studies of face perception in humans. *Journal of Cognitive Neuroscience*, *8*(6), 551–565. https://doi.org/10.1162/jocn.1996.8.6.551

Binder, M. D., Hirokawa, N., & Windhorst, U. (2009). Superior prefrontal gyrus. In M. D. Binder, N. Hirokawa, & U. Windhorst (Eds.), *Encyclopedia of neuroscience* (pp. 3896). Springer Berlin Heidelberg. https://doi.org/10.1007/978-3-540-29678-2_5755

Binnie, C. D., & Prior, P. F. (1994). Electroencephalography. *Journal of Neurology, Neurosurgery, and Psychiatry*, *57*, 1308–1319.

Bland, B. H., Jackson, J., Derrie-Gillespie, D., Azad, T., Rickhi, A., & Abriam, J. (2006). Amplitude, Frequency, and Phase Analysis of Hippocampal Theta During Sensorimotor Processing in a Jump Avoidance Task. *Hippocampus*, *16*, 673–681. https://doi.org/10.1002/hipo

Blau, V. C., Maurer, U., Tottenham, N., & McCandliss, B. D. (2007). The face-specific N170 component is modulated by emotional facial expression. *Behavioral and Brain Functions*, *3*, 1–13. https://doi.org/10.1186/1744-9081-3-7

Bookheimer, S. Y. (2013). Precentral gyrus. In F. R. Volkmar (Ed.), *Encyclopedia of autism spectrum disorders* (pp. 2334–2335). Springer New York. https://doi.org/10.1007/978-1-4419-1698-3_203

Brown, L. E., Halpert, B. A., & Goodale, M. A. (2005). Peripheral vision for perception and action. *Experimental Brain Research*, *165*(1), 97–106. https://doi.org/10.1007/s00221-005-2285-y

Cohen, N. R., Cross, E. S., Tunik, E., Grafton, S. T., & Culham, J. C. (2009). Ventral and dorsal stream contributions to the online control of immediate and delayed grasping: A TMS approach. *Neuropsychologia*, *47*(6), 1553–1562. https://doi.org/10.1016/j.neuropsychologia.2008.12.034

Crick, F., & Jones, E. (1993). Backwardness of human neuroanatomy. *Nature*, *361*(6408), 109–110. https://doi.org/10.1038/361109a0

Cruikshank, L. C., Caplan, J. B., & Singhal, A. (2012a). Human electrophysiological reflections of the recruitment of perceptual processing during actions that engage memory. *Journal of Vision, 12(6),* 1–13. https://doi.org/10.1167/12.6.29

Cruikshank, L. C., Caplan, J. B., & Singhal, A. (2014). A perception-based ERP reveals that the magnitude of delay matters for memory-guided reaching. *Experimental Brain Research*, *232*(7), 2087–2094. https://doi.org/10.1007/s00221-014-3897-x

Cruikshank, L. C., Singhal, A., Hueppelsheuser, M., & Caplan, J. B. (2012b). Theta oscillations reflect a putative neural mechanism for human sensorimotor integration. *Journal of Neurophysiology*, *107*(1), 65–77. https://doi.org/10.1152/jn.00893.2010

Danckert, J., & Goodale, M. A. (2001). Superior performance for visually guided pointing in the lower visual field. *Experimental Brain Research*, *137*(3–4), 303–308. https://doi.org/10.1007/s002210000653

Dewar, M. T., & Carey, D. P. (2006). Visuomotor “immunity” to perceptual illusion: A mismatch of attentional demands cannot explain the perception-action dissociation. *Neuropsychologia*, *44*(8), 1501–1508. https://doi.org/10.1016/j.neuropsychologia.2005.11.010

Dijkerman, H. C., Milner, A. D., & Carey, D. P. (1998). Grasping Spatial Relationships: Failure to Demonstrate Allocentric Visual Coding in a Patient with Visual Form Agnosia. *Consciousness and Cognition*, *7*(3), 424–437. https://doi.org/10.1006/ccog.1998.0365

Eimer, M. (2000). The face-specific N170 component reflects late stages in the structural encoding of faces. *NeuroReport*, *11*(10), 2319–2324. https://doi.org/10.1097/00001756-200007140-00050

Eimer, M. (2012). The face-sensitive n170 component of the event-related brain potential. In G. Rhodes, A. Calder, M. Johnson, & J.V. Haxby (Eds.), *Oxford Handbook of Face Perception* (pp. 329–344). Oxford University Press. https://doi.org/10.1093/oxfordhb/9780199559053.013.0017

Ferber, S., Humphrey, G. K., & Vilis, T. (2003). The lateral occipital complex subserves the perceptual persistence of motion-defined groupings. *Cerebral Cortex*, *13*(7), 716–721. https://doi.org/10.1093/cercor/13.7.716

Franz, V. H., Hesse, C., & Kollath, S. (2009). Visual illusions, delayed grasping, and memory: No shift from dorsal to ventral control. *Neuropsychologia*, *47*(6), 1518–1531. https://doi.org/10.1016/j.neuropsychologia.2008.08.029

Glover, G. H. (2011). Overview of functional magnetic resonance imaging. *Neurosurgery*

Clinics of North America, *22*(2), 133–139. https://doi.org/10.1016/j.nec.2010.11.001

Gonzalez, C. L. R., Ganel, T., & Goodale, M. A. (2006). Hemispheric specialization for the visual control of action is independent of handedness. *Journal of Neurophysiology*, *95*(6), 3496–3501. https://doi.org/10.1152/jn.01187.2005

Goodale, M. A. (1998). Vision for perception and vision for action in the primate brain. In G. R. Bock & J. A. Goode (Eds.), *Sensory guidance of movment novartis foundation symposium 218* (pp. 21–39). John Wiley & Sons.

Goodale, M. A. (2014). How (and why) the visual control of action differs from visual perception. *Proceedings of the Royal Society B: Biological Sciences*, *281*(1785), 1–9. https://doi.org/10.1098/rspb.2014.0337

Goodale, M. A., & Humphrey, G. K. (1998). The objects of action and perception. *Cognition*, *67*, 181–207.

Goodale, M. A., Jakobson, L. S., & Keillor, J. M. (1994). Differences in the visual control of pantomimed and natural grasping movements. *Neuropsychologia*, *32*(10), 1159–1178. https://doi.org/10.1016/0028-3932(94)90100-7

Goodale, M. A., & Milner, A. D. (1992). Separate visual pathways for perception and action. *Trends in Neurosciences*, *15*(1), 20–25. https://doi.org/10.1093/litthe/11.1.80

Goodale, M. A., Milner, A. D., Jakobson, L. S., & Carey, D. P. (1991). A neurological dissociation between perceiving objects and grasping them. *Nature*, *349*, 154–156.

Goodale, M. A., Westwood, D. A., & Milner, A. D. (2004). Two distinct modes of control for object-directed action. *Progress in Brain Research*, *144*, 131–144. https://doi.org/10.1016/S0079-6123(03)14409-3

Grill-Spector, K., Kourtzi, Z., & Kanwisher, N. (2001). The lateral occipital complex and its role in object recognition. *Vision Research*, *41*(10–11), 1409–1422. https://doi.org/10.1016/S0042-6989(01)00073-6

Haffenden, A. M., & Goodale, M. A. (1998). The effect of pictorial illusion on perception and visually guided prehension. *Investigative Ophthalmology and Visual Science*, *37*(3), 122–136.

Handy, T. C., Grafton, S. T., Shroff, N. M., Ketay, S., & Gazzaniga, M. S. (2003). Graspable objects grab attention when the potential for action is recognized. *Nature Neuroscience*, *6*(4), 421–427. https://doi.org/10.1038/nn1031

Hesse, C., & Franz, V. H. (2009). Memory mechanisms in grasping. *Neuropsychologia*, *47*(6), 1532–1545. https://doi.org/10.1016/j.neuropsychologia.2008.08.012

James, T. W., Culham, J., Humphrey, G. K., Milner, A. D., & Goodale, M. A. (2003). Ventral occipital lesions impair object recognition but not object-directed grasping: An fMRI study. *Brain*, *126*(11), 2463–2475. https://doi.org/10.1093/brain/awg248

Krigolson, O., & Heath, M. (2004). Background visual cues and memory-guided reaching. *Human Movement Science*, *23*(6), 861–877. https://doi.org/10.1016/j.humov.2004.10.011

Le, A., & Niemeier, M. (2014). Visual field preferences of object analysis for grasping with one hand. *Frontiers in Human Neuroscience*, *8*(762), 1–12. https://doi.org/10.3389/fnhum.2014.00782

Luck, S. J. (2005). An introduction to event-related potentials and their neural origins. In S. J. Luck (Ed.), *An introduction to the event-related potential technique* (1st ed., pp. 1–50). A Bradford Book.

Machado, S., Cunha, M., Velasques, B., Minc, D., Teixeira, S., Domingues, C. A., Silva, J. G., Bastos, V. H., Budde, H., Cagy, M., Basile, L., Piedade, R., & Ribeiro, P. (2010).

Sensorimotor integration: basic concepts, abnormalities related to movement disorders and sensorimotor training-induced cortical reorganization. *Revista de Neurologia*, *51*(7), 427–436. https://doi.org/10.33588/rn.5107.2010228

Milner, A. D., Dijkerman, H. C., Pisella, L., McIntosh, R. D., Tilikete, C., Vighetto, A., & Rossetti, Y. (2001). Grasping the past: Delay can improve visuomotor performance. *Current Biology*, *11*(23), 1896–1901. https://doi.org/10.1016/S0960-9822(01)00591-7

Milner, A. D., & Goodale, M. A. (2006). Visual processing in the primate visual cortex. In M. D'Esposito, D. Schacter, J. Driver, A. Treisman, T. Robbins, & L. Weiskrantz (Eds.), *The visual brain in action* (2nd ed., pp. 1–39). Oxford University Press. https://doi.org/10.1093/acprof:oso/9780198524724.003.0002

Mishkin, M., Ungerleider, L. G., & Macko, K. A. (1983). Object vision and spatial vision: two cortical pathways. *Trends in Neurosciences*, *6*, 414–417. https://doi.org/10.1016/0166-2236(83)90190-X

Newcombe, F., Ratcliff, G., & Damasio, H. (1987). Dissociable visual and spatial impairments following right posterior cerebral lesions: Clinical, neuropsychological and anatomical evidence. *Neuropsychologia*, *25*(1B), 149–161. https://doi.org/10.1016/0028-3932(87)90127-8

Radoeva, P. D., Cohen, J. D., Corballis, P. M., Lukovits, T. G., & Koleva, S. G. (2005). Hemispheric asymmetry in a dissociation between the visuomotor and visuoperceptual streams. *Neuropsychologia*, *43*(12), 1763–1773. https://doi.org/10.1016/j.neuropsychologia.2005.02.005

Rossion, B., Joyce, C. A., Cottrell, G. W., & Tarr, M. J. (2003). Early lateralization and orientation tuning for face, word, and object processing in the visual cortex. *NeuroImage*, *20*(3), 1609–1624. https://doi.org/10.1016/j.neuroimage.2003.07.010

Rossit, S., McAdam, T., Mclean, D. A., Goodale, M. A., & Culham, J. C. (2013). FMRI reveals a lower visual field preference for hand actions in human superior parieto-occipital cortex (SPOC) and precuneus. *Cortex*, *49*(9), 2525–2541. https://doi.org/10.1016/j.cortex.2012.12.014

Singhal, A., Chinellato, E., Culham, J. C., & Goodale, M. A. (2007). Dual-task interference is greater in memory-guided grasping than in visually guided grasping. *Journal of Vision*, 7(5), 1–12. http://journalofvision.org/7/5/5/, doi:10.1167/7.5.5.

Singhal, A., Monaco, S., Kaufman, L. D., & Culham, J. C. (2013). Human fMRI Reveals That Delayed Action Re-Recruits Visual Perception. *PLoS ONE*, *8*(9):e73629. https://doi.org/10.1371/journal.pone.0073629

Westwood, D. A., & Goodale, M. A. (2003). Perceptual illusion and the real-time control of action. *Spatial Vision*, *16*(3–4), 243–254. https://doi.org/10.1163/156856803322467518

Westwood, D. A., Heath, M., & Roy, E. A. (2000). The effect of a pictorial illusion on closed-loop and open-loop prehension. *Experimental Brain Research*, *134*(4), 456–463. https://doi.org/10.1007/s002210000489

Westwood, D. A., Heath, M., & Roy, E. A. (2001a). The accuracy of reaching movements in brief delay conditions. *Canadian Journal of Experimental Psychology*, *55*(4), 304–310. https://doi.org/10.1037/h0087377

Westwood, D. A., McEachern, T., & Roy, E. A. (2001b). Delayed grasping of a Müller-Lyer figure. *Experimental Brain Research*, *141*(2), 166–173. https://doi.org/10.1007/s002210100865

Woodman, G. F. (2010). A brief introduction to use of ERPs in studies of perception and attention. *Attention, Perception, & Psychophysics*, *72*(8), 1–29.

https://doi.org/10.3758/APP.72.8.2031.A

Appendix A

Post-hoc Analysis: Multiple Bins

Nevertheless, there may be a second explanation for the morphological pattern of the memory-guided N170 ERPs at T5. From a structural standpoint, the most obvious thing is that bins 1 and 4 are surrounded by an upper and lower border while bins 2 and 3 are not. These borders are visual spatial cues which are known to facilitate online control of both delayed and immediate actions (Krigolson & Heath, 2004). Perhaps in our experiment, these borders are somehow interfering with the movement planning in the memory-guided condition. Therefore, delayed actions at bins 1 and 4 may require more perceptual effort, and the N170 ERPs at these bins are reflecting a border effect. To test this possibility, we undertook a post-hoc analysis and manipulated the number of bins using three factors of 360 (3 bins, 6 bins and 8 bins) for both trial types. Recall that there are 360 total trials, and to ensure equal distribution of trials per condition and bin we must use factors of 360. For this post-hoc analysis however, we did not perform any statistical tests. If the N170 ERPs in the memory-guided condition are being influenced by the border, then we expect to see the u-function at 4 bins recreated for the 3, 6 and 8 bin configurations. Specifically, the N170 ERPs for the upper and lower most bins will peak together and be more negative-going, while the ERPs for the remainder of the bins will accumulate together closer to the baseline. This is because the upper and lower most bins will always remain surrounded by a border regardless of how the total number of bins are divided. On the other hand, if the border is not affecting the N170 ERPs, then the morphological pattern of the waveforms will not resemble each other at any bin configuration.

As evident in Appendix D, the post-hoc analysis only revealed a u-function for the memory-guided ERPs. It is important to point out that as the bin count is increasing from 3 to 8 bins, the waveforms are becoming progressively noisier. This is to be expected because there are fewer trials averaged into each bin with increasing bin number, which will result in a noisier measure. This means that in the 3 bin configuration there are going to be most amount of trials averaged into each bin, because each individual bin takes up more screen space. Additionally, as the number of bins increase from 3 bins to 8 bins, there are going to be fewer and fewer trials averaged into each bin because each individual bin takes up less and less screen space. Nevertheless, for the 3 bin arrangement, the u-function in the N170 ERPs looks like that at 4 bins. Though this u-function changes as the bins are increased to 6 bins and 8 bins. For these bin counts, the N170 ERPs are identically peaking for the two upper and lowermost bins. In other words, bins 1 and 2 are peaking with bins 5 and 6 in the 6 bin configuration, whereas bins 1 and 2 are peaking with bins 7 and 8 for the 8 bin arrangement. For this reason, a border effect cannot fully explain the patterns in the ERPs at 6 and 8 bins. Instead, the two upper and lowermost bins for the 6 and 8 bin configurations likely represent upper and lower visual fields. This trend likely materialized only in the 6 and 8 bin arrangements, simply because the bins are generally smaller and occupy less screen space. Conversely, the bins are fundamentally larger in the 3 and 4 bin formations and fill more of the screen, which are thereby hiding this small pattern. The results of the post-hoc analysis seems to support the visual field account proposed earlier. Therefore, the morphological pattern at bins 1 and 4 in the 4 bin configuration, is likely representing memory-guided reaching in the upper and lower visual fields. That said, we are not able to fully rule out a border effect since the border is still a spatial cue. In some capacity, the upper and lower borders of the screen are sure to influence movement planning of delayed actions although it is not clear in what manner and to what degree. It is also challenging to directly test such a possibility considering our current paradigm. Once again, further research into how visual spatial cues affect delayed actions at variable reach-heights is necessary. Lastly, in the visually-guided condition the post-hoc analysis elucidated no u-function and the ERPs look unchanged.

In Appendix E, the post-hoc analysis demonstrated no u-function at T6. Indeed, regardless of the bin count there are still no differences between conditions even with the increased noise at the 6 and 8 bin formations. Overall, arbitrarily manipulating the bin count reliably replicates no differences between conditions. These results further strengthen our argument that there may not truly be reach type differences in the right hemisphere. Despite no main effects of reach-height at either electrode, there is still good consistency between our two central ERP analyses. Most notably, we managed to replicate a larger N170 difference between conditions at T5 and no differences at T6, regardless if the ERPs were binned or unbinned.

Appendix B

Post-hoc Analysis: Horizontal Bins

One thing we sought to gain more insight into, was for the best or better interpretation of our main reach-height results. As discussed earlier, the main effects of reach-height were non-significant for both conditions at both T5 and T6. However, it is unclear if this is because our dataset is not sensitive enough to identify an effect of bins. In order to directly test this, we undertook a secondary post-hoc analysis and measured the N170 ERP for memory and visually-guided actions to targets presented across the left and right visual fields. This serves as a good control comparison, because although we are comparing hand actions across the left and right visual fields, the experimental design remains unchanged. If there is an effect of horizontal bins on the N170 ERP at either electrode, this suggests our dataset is indeed sensitive to detect an effect of bins and our main reach-height results should be viewed more as null effects. This is because we cannot fully attribute the absence of a main effect of reach-height, due to the lack of sensitivity in the dataset. Alternatively, revealing no effect of horizontal bins would suggest that perhaps our dataset is not sensitive to detect an effect of bins in either the vertical or horizontal direction. In other words, we should view both the main effects of horizontal and vertical bins as null effects. Once again, target location was randomly drawn from a uniform distribution in the horizontal dimension. Following this, we then calculated the range of pixel values across the horizontal dimension, and then segmented the touch screen into four equal "horizontal bins" from left to right, representing different lateral positions for the subject to reach to. These horizontal bins are ordered from one to four in order of increasing ipsilaterality with respect to the right side of the screen. That is, horizontal bin 1 represents the left and contralateral most bin, whereas horizontal bin 4 represents the right-most ipsilateral bin. It is significant to mention that there is a much narrower range of pixel values in the horizontal dimension, because the distance between the lateral borders is much smaller than the distance between the upper and lower borders. The three ERP measures (Time-Window Mean Amplitude, Minimum Amplitude and Latency) were quantified and kept identical to those of the vertical bins and extracted over a window between 150 ms – 300 ms. Similarly, all ERP measures were averaged across all conditions, trials and horizontal bins and analyzed using a reach type [2] (visually guided/memory-guided) X laterality [4] (horizontal bin 1/horizontal bin 2/ horizontal bin 3/horizontal bin 4) repeated-measures ANOVA. Grand-average ERP waveforms are shown horizontally binned for both trial types separately at each individual electrode in Appendix F. Additionally, descriptive statistics and classical ANOVA outputs for all ERP measures at each temporal electrode are reported in Appendix G – H for T5 and I – J for T6.

At T5, the ANOVA only revealed main effects of condition on the N170 time-window mean amplitude and minimum amplitude (Appendix F, Appendix H). Specifically, the N170 ERP time-window mean amplitude is +0.63 µV more positive with overall more positive voltage values across the entire time window for the visually-guided condition than the memory-guided condition. In the same vein, the N170 minimum amplitude is -1.00 µV more negative in the memory-guided trials than in the visually-guided trials. At T6 however, the main effect of condition failed to reach significance for all ERP measures (Appendix F, Appendix J). Together, these findings directly replicate our unbinned ERP analyses and further strengthen the conclusion that the left hemisphere may be specialized for memory-guided actions in right-handed people. This is because trial type differences in the left hemisphere and lack thereof in the right hemisphere remain preserved, regardless if the ERPs are unbinned, binned vertically or binned horizontally. Finally, at T5 there were no main effects of laterality on any of the three ERP measures. In the visually-guided condition, all the ERPs appear to be collectively accumulating around the baseline, with the exception of the N170 ERP at horizontal bin 2 which exceeds the baseline in the positive direction. The non-significant trend of these waveforms seems to be similar to that of the previously cited visually-guided waveforms for the vertical bins. In particular, the ‘P150’ is once again present, and not only coincides with but also endures a lot longer than the actual N170 across all horizontal bins. This positive source is sure to drive all the voltage values more positively and this will be the most prominent at horizontal bin 2 given that is has the most positive-going peak. Indeed, the ERPs in the immediate reaching condition may not reflect any differences in lateral reaches but could be the result of the ‘P150’ influencing the voltage values in a more positive direction. In the delayed condition, the waveforms for horizontal bins 1 – 3 are all peaking together and near the baseline, whereas the ERP for horizontal bin 4 peaks separate from the rest and is also more negative. The non-significant trend in the memory-guided waveforms seems relatively consistent with the idea that there is greater sensitivity to targets presented in the right visual field than the left-visual field for right-handed participants (Handy et al., 2003; Le & Niemeier, 2014). Recall that horizontal bins 1 and 2 are on the left side of the screen, whereas horizontal bins 3 and 4 are on the right side of the screen. Therefore, pointing actions to targets in horizontal bins 1 – 2 and horizontal bins 3 – 4, presumably represent hand actions performed in the left and right visual-fields, respectively. The morphological pattern of the memory-guided waveforms is not fully aligned with this notion however because the ERPs at horizontal bins 3 and 4 did not peak together, and they presumably reflect the right-visual field. This could be because targets are more centralized at horizontal bin 3 than horizontal bin 4 which is on the right most side of the screen. Perhaps there is less sensitivity, or the sensitivity is more subtle to targets at horizontal bin 3 because they are more centralized compared to those at horizontal bin 4. Nevertheless, the N170 ERP at horizontal bin 4 could be larger because the targets are being presented within some portion of the right-visual field and may not necessarily reflect an increase in perceptual effort for memory-guided actions in the right-visual field. Lastly, comparing the horizontal binned ERPs across conditions reveals no other distinct morphological patterns.

At T6 surprisingly, the ANOVA revealed a main effect of horizontal bins only on the time-window mean amplitude of the N170 (Appendix J). Across both conditions, the ERPS at horizontal bins 1 and 2 are peaking together and closer to baseline while the waveforms at bins 3 and 4 are also peaking together and are more negative (Appendix F). Moreover, the ERPs are at least -0.78 μV more negative at horizontal bins 3 – 4 than they are at horizontal bins 1 – 2. This result is surprising because in our main reach-height analyses we predicted the main effect to be in the vertical direction, and therefore manipulated the range of variability more in the vertical axis than in the horizontal axis. The main effect of horizontal bins is all the more impressive because the range of movements in the horizontal direction are much narrower, yet we still found an effect of bins and this effect on the N170 ERP is larger. As previously mentioned, our main analyses sought to investigate the effect of reach-height on the N170 ERP of both delayed and immediate actions. In that respect, the main effect of horizontal bins solidifies our interpretation that the effect of reach-height is indeed null or that it may be smaller or harder to detect than the difference present in the horizontal direction. Essentially, this analysis, demonstrates that the properties of the data we have are indeed sensitive to detect an effect of bins. However, because the main effect of bins in the horizontal direction is so robust, it may be telling us something new about hand actions across the left and right visual fields. Namely, the ERPs are smaller in magnitude in the right-visual field and larger in magnitude in the left-visual field for both delayed and immediate actions. This replicates previous behavioral work done in our lab, by Atkin and Singhal (In Preparation), which found that ipsilateral hand actions have better performance than contralateral hand actions. In their study, right-hand dominant participants were instructed to reach towards lateral targets presented in a horizontal array using either their left or right hands. One of the main findings from that experiment was that performance of right-handed actions was better to targets in the ipsilateral visual field than in the contralateral visual field. That is to say, right-handed pointing actions are performed better in the right-visual field than in the left-visual field. In addition, right-handed subjects would also generally choose to utilize their left-hands for targets in the left-visual field. It is thought that there is a preference for executing hand actions in the ipsilateral visual field (Le & Niemeier, 2014), presumably because there is less motor planning and biomechanical demand involved than hand actions in the contralateral visual field. Though we did not manipulate handedness, our effect of horizontal bins at T6 seems to be in conformity with the results of Atkin and Singhal (In Preperation). For memory-guided actions, the movement programming of ipsilateral reaches is likely easier because it is less biomechanically complex and thus less perceptual processing is required. By contrast, contralateral delayed actions presumably require increased perceptual mechanisms because there is crossing of the body involved and therefore may be more biomechanically demanding. This suggests that in the right-hemisphere there may be greater contribution of the ventral stream for contralateral memory-guided reaches than ipsilateral ones. Interestingly, for the visually-guided trial, we can also observe that the N170 ERPs are larger in the contralateral left visual field than the ipsilateral right visual field. This indicates that similarly in the right hemisphere, visually-guided actions to the contralateral side of the screen are somehow also reliant on the ventral stream. Given the novelty of our findings, it is evident that more detailed analyses are required to better clarify the role of right hemisphere ventral stream mechanisms in delayed and potentially immediate actions for the left and right visual fields. Perhaps we only revealed a main effect of horizontal bins because of competition for the left hand in the left-visual field. Simply stated, maybe the increase in the amplitude of the N170 is not reflecting an increase in perceptual effort, but is because right-handers naturally prefer to use their left and not their right hand in the left-visual field for both memory and visually-guided actions.

Overall, the ERP results for the horizontal bins analysis are consistent with our earlier ERP analysis and offer some novel findings. Mainly, there were differences between conditions at T5 but not T6 across the unbinned, vertically binned and horizontally binned ERPs. By the same token, we revealed a main effect of laterality at T6, which was not found at T5. Our results at T5 provide further evidence that the left-hemisphere may be specialized for delayed actions. Likewise, our findings at T6 support previous work by our lab group (Atkin and Singhal, In Preparation), indicating that in the right hemisphere delayed and immediate actions may be benefitted in the right visual field but not the left visual field.

Appendix C

Post-hoc Analysis: Topographic Plots

Our last post-hoc analysis revolved around creating topographic plots for the vertical bins of both conditions and to try and intersect the patterns in the topographic plots with those of the N170 ERP waveforms at T5 and T6. A topographic plot allows the visualization of voltage values at all electrodes given a specified range of time points, which in this case we specified between 150 ms – 300 ms. This is different from ERP waveforms which display the voltage values for all time points at one specified electrode. By analyzing the ERP waveforms at T5 and T6 alongside the topographic plots, it will allow us to better understand the underlying neural mechanisms across conditions and vertical bins. For the visually-guided condition across all the vertical bins, the topographic plots show that T5 has positive voltage values that are becoming increasingly more positive from vertical bins 1 – 4, whereas at T6 the voltage values are remaining steadily negative across all vertical bins (Appendix K). The patterns of activity at T5 and T6 across the vertical bins seem to be in-line with the non-significant morphological patterns of the visually-guided ERPs at these electrodes. Recall, at T5 the visually-guided ERPs were progressively becoming more positive across vertical bins, whereas at T6 the waveforms were more negative with no noticeable differences across vertical bins. Additionally, another observable pattern in the visually-guided topographic plots, is that there is a dipole at midline areas and there seems to be overall more positive voltage values in the left hemisphere than in the right hemisphere all the vertical bins. This indicates that the dipole may be moving from one hemisphere to the other in either direction. Likewise, in the memory-guided condition we can observe these similar patterns of activity that persist across all the vertical bins. At T5 the topographic plots demonstrate more negative voltage values at vertical bins 1 and 4 and positive voltage values at vertical bins 2 – 3 (Appendix L). However, at T6 the voltage values are all constantly negative with no differences across vertical bins (Appendix L). The patterns of activation at T5 and T6 corroborate the non-significant trend in the memory-guided ERPs at these respective electrodes. This is because at T5 the memory-guided waveforms were the most negative-going at vertical bins 1 – 4, while at vertical bins 2 – 3 the ERPs were more positive-going. However, at T6, all the memory-guided ERPs peaked simultaneously with no differences across vertical bins. Furthermore, there appears to be a dipole originating at midline cortical areas and there are more positive voltage values in the left-hemisphere and more negative voltage values in the right hemisphere. This suggests that the dipole may once again be traveling from the left-hemisphere to the right-hemisphere or vice versa.

Interestingly, when we compare the topographic plots across conditions there is another pattern that emerges. In particular, the memory-guided topographic plots reveal the strongest activation in more frontal and midline cortical areas, while the visually-guided topographic plots have more activation in midline and posterior parietal-occipital areas. In addition, these different patterns of activation for both conditions become increasingly more robust across the vertical bins. If you approximate the current dipole patterns of activation at the midline for the memory-guided condition it looks like the activation is somewhere in the precentral and superior frontal gyri. The precentral gyrus houses the primary motor cortex which is thought to be responsible for executing voluntary movements, while the superior frontal gyri is thought to help with motor planning of these voluntary movements (Binder et al., 2009; Bookheimer, 2013). One interpretation is that memory-guided reaching may require more motor planning at higher reaches, which is why there is more activation in frontal and midline areas when compared to visually-guided reaching. It is likely that delayed actions to higher targets are more biomechanically complex than immediate actions, and therefore more movement programming is required. Additionally, there appears to be increased activation in posterior parietal-occipital areas for visually-guided actions to higher target positions, that is not present in the memory-guided topographic plots. Perhaps the greater activation in these areas for the visually-guided actions is reflecting increased contribution from parietal-occipital cortical areas, which are known to be more involved in mediating immediate actions than delayed actions (Goodale & Milner, 1992). In sum, the activation patterns in the topographic plots support the morphological patterns of the ERPs for both conditions across all the vertical bins. However, the topographic plots demonstrate that for both conditions the pattern of activations was the strongest at midline and parietal-occipital areas and not around temporal areas such as T5 and T6. This suggests that the N170 may not be as robust at temporal sites as initially thought and it may be worth exploring this ERP in more midline and parietal-occipital electrodes in future analyses.

Appendix D

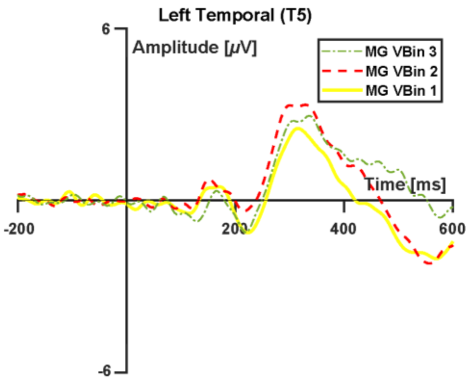
Left Temporal (T5)
6
Amplitude [μV]
MG VBin 3
MG VBin 2
MG VBin 1
Time [ms]
-200
200
400
600
-6

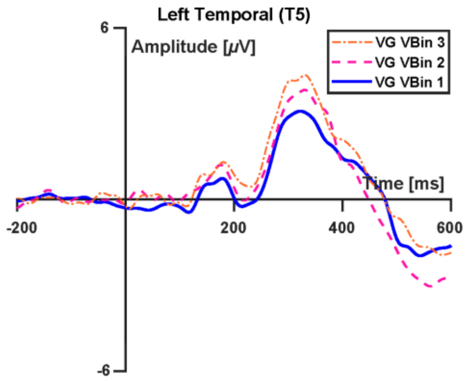
Left Temporal (T5)
6
Amplitude [μV]
VG VBin 3
VG VBin 2
VG VBin 1
Time [ms]
-200
200
400
600
-6

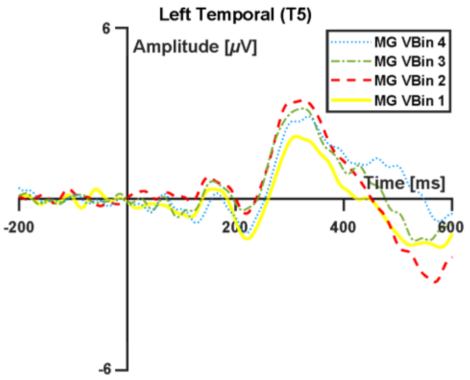
Left Temporal (T5)
6
Amplitude [μV]
MG VBin 4
MG VBin 3
MG VBin 2
MG VBin 1
Time [ms]
-200
200
400
600
-6

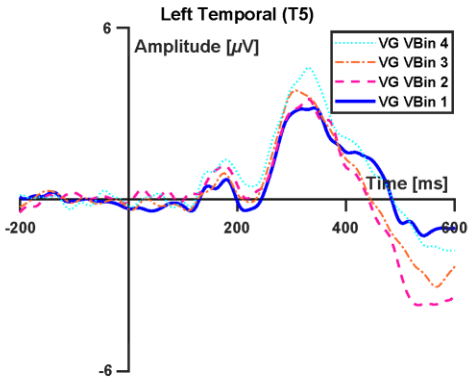
Left Temporal (T5)
6
Amplitude [μV]
VG VBin 4
VG VBin 3
VG VBin 2
VG VBin 1
Time [ms]
-200
200
400
600
-6

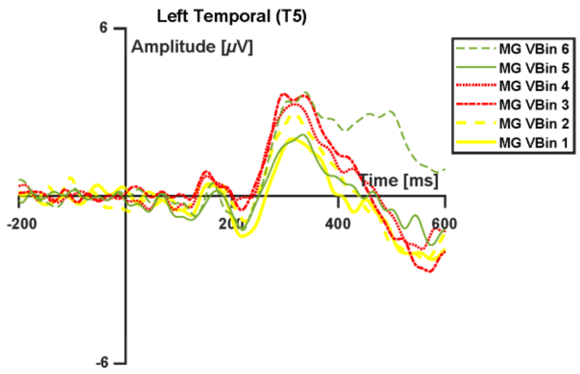
Left Temporal (T5)
6
Amplitude [μV]
MG VBin 6
MG VBin 5
MG VBin 4
MG VBin 3
MG VBin 2
MG VBin 1
Time [ms]
-200
200
400
600
-6

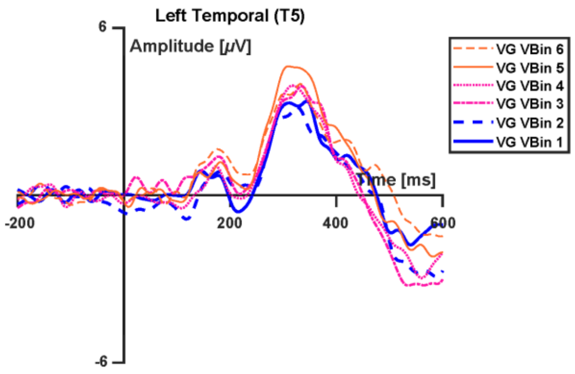
Left Temporal (T5)
6
Amplitude [μV]
VG VBin 6
VG VBin 5
VG VBin 4
VG VBin 3
VG VBin 2
VG VBin 1
Time [ms]
-200
200
400
600
-6

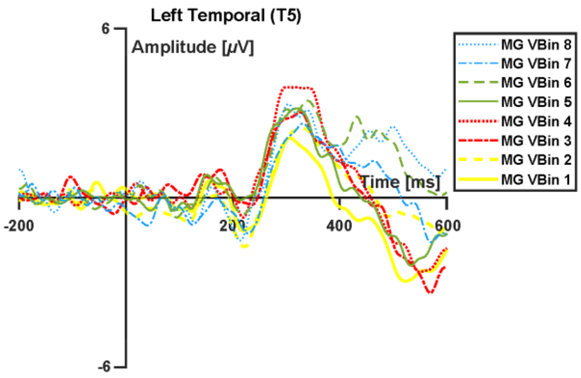
Left Temporal (T5)
6
Amplitude [μV]
MG VBin 8
MG VBin 7
MG VBin 6
MG VBin 5
MG VBin 4
MG VBin 3
MG VBin 2
MG VBin 1
Time [ms]
-200
200
400
600
-6

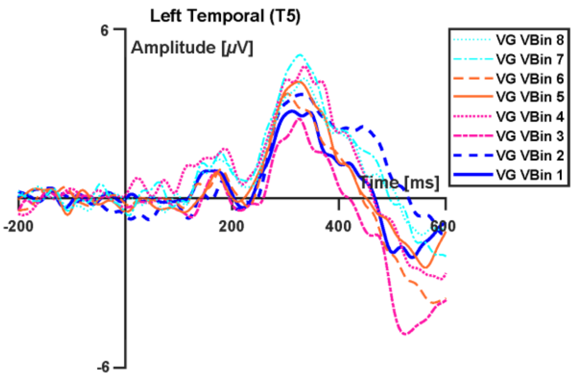
Left Temporal (T5)
6
Amplitude [μV]
VG VBin 8
VG VBin 7
VG VBin 6
VG VBin 5
VG VBin 4
VG VBin 3
VG VBin 2
VG VBin 1
Time [ms]
-200
200
400
600
-6

Appendix D Caption:

N170 ERP waveforms grand averaged and binned vertically for the memory-guided (MG) and visually-guided (VG) test conditions only at the contralateral temporal electrode, T5. Time (ms) is plotted on the x-axis and amplitude (µV) is plotted on the y-axis. The following N170 ERP waveforms are binned in differing factors of 360, starting with 3 and ending with 8. Across all the binned figures, all individual N170 waveforms have been colorized separately to facilitate easier identification. Please note, the binned ERPs that use 4 bins are the same ERPs shown previously and have been added here for comparison.

Appendix E

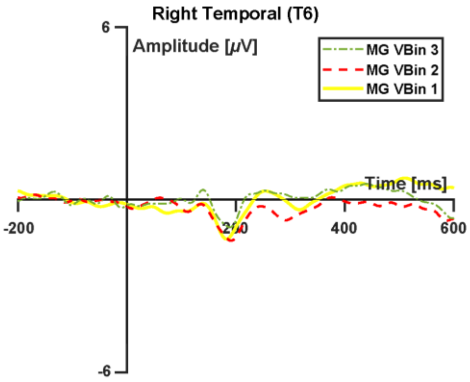
Right Temporal (T6)
Amplitude [μV]
Time [ms]
6
-6
-200
200
400
600
MG VBin 3
MG VBin 2
MG VBin 1

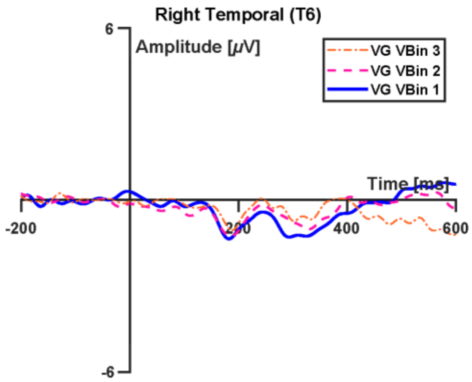
Right Temporal (T6)
Amplitude [μV]
Time [ms]
6
-6
-200
200
400
600
VG VBin 3
VG VBin 2
VG VBin 1

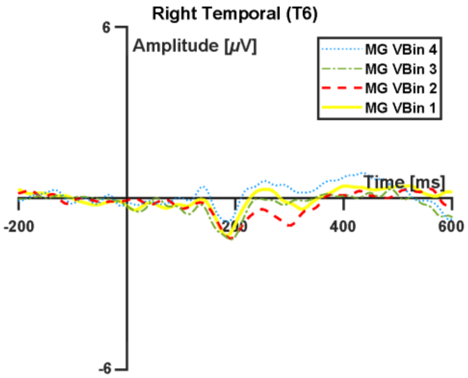
Right Temporal (T6)
Amplitude [μV]
Time [ms]
6
-6
-200
200
400
600
MG VBin 4
MG VBin 3
MG VBin 2
MG VBin 1

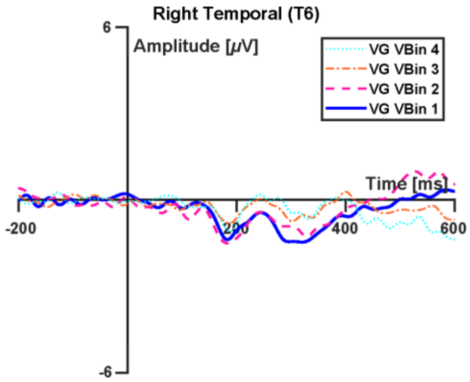
Right Temporal (T6)
Amplitude [μV]
Time [ms]
6
-6
-200
200
400
600
VG VBin 4
VG VBin 3
VG VBin 2
VG VBin 1

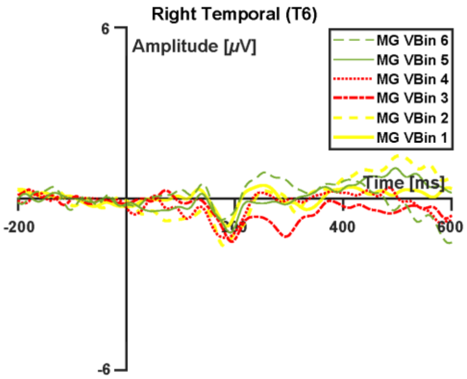
Right Temporal (T6)
Amplitude [μV]
Time [ms]
6
-6
-200
200
400
600
MG VBin 6
MG VBin 5
MG VBin 4
MG VBin 3
MG VBin 2
MG VBin 1

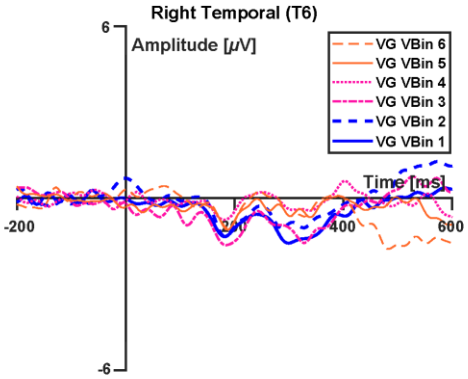
Right Temporal (T6)
Amplitude [μV]
Time [ms]
6
-6
-200
200
400
600
VG VBin 6
VG VBin 5
VG VBin 4
VG VBin 3
VG VBin 2
VG VBin 1

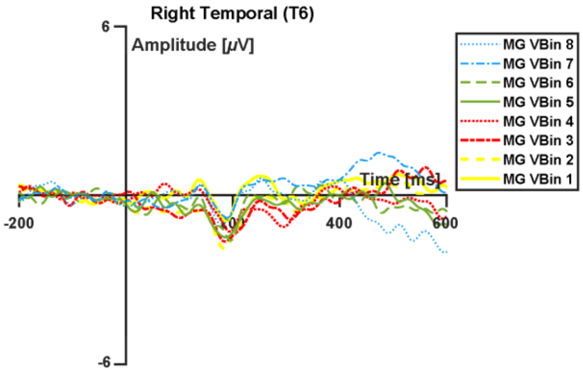
Right Temporal (T6)
Amplitude [μV]
Time [ms]
6
-6
-200
200
400
600
MG VBin 8
MG VBin 7
MG VBin 6
MG VBin 5
MG VBin 4
MG VBin 3
MG VBin 2
MG VBin 1

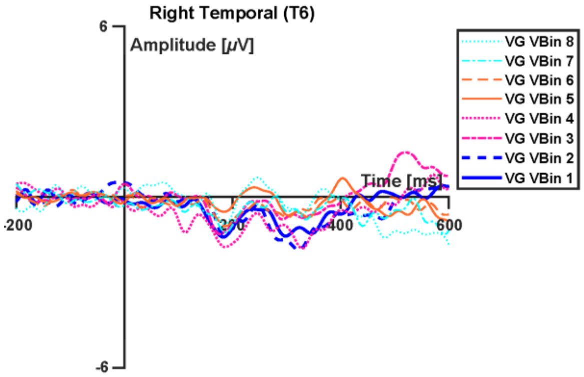
Right Temporal (T6)
Amplitude [μV]
Time [ms]
6
-6
-200
200
400
600
VG VBin 8
VG VBin 7
VG VBin 6
VG VBin 5
VG VBin 4
VG VBin 3
VG VBin 2
VG VBin 1

Appendix E Caption:

N170 ERP waveforms grand averaged and binned vertically for the memory-guided (MG) and visually-guided (VG) test conditions only at the ipsilateral temporal electrode, T6. Time (ms) is plotted on the x-axis and amplitude (μV) is plotted on the y-axis. The following N170 ERP waveforms are binned in differing factors of 360, starting with 3 and ending with 8. Across all the binned figures, all individual N170 waveforms have been colorized separately to facilitate easier identification. Please note, the binned ERPs that use 4 bins are the same ERPs shown previously and have been added here for comparison.

Appendix F

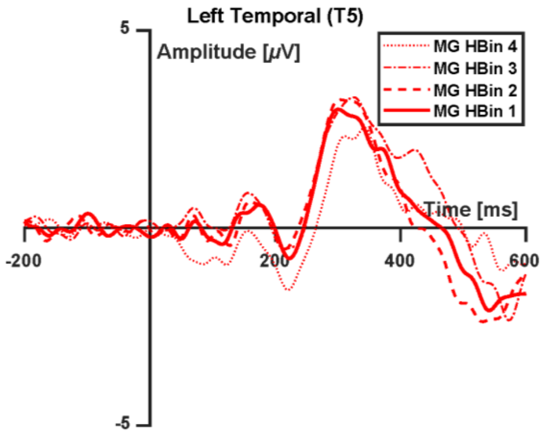
Left Temporal (T5)

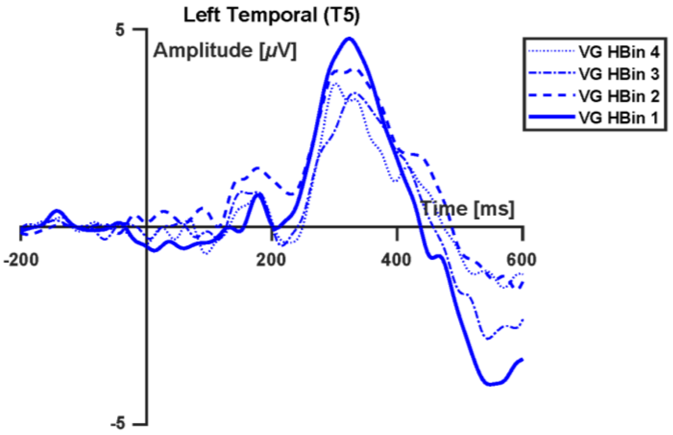
Left Temporal (T5)

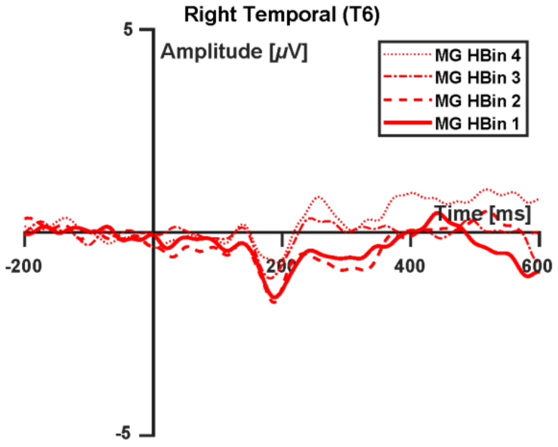
Right Temporal (T6)

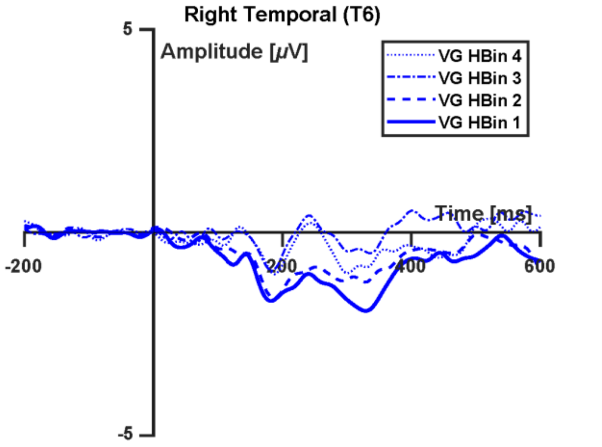
Right Temporal (T6)

Appendix F Caption:

Top Two Panels: N170 ERP waveforms grand averaged and binned horizontally for the memory-guided (MG) and visually-guided (VG) test conditions. The bins are now segmented from left to right, with bin 1 – 4 increasing ipsilaterally towards the right side, only at the contralateral temporal electrode, T5. Time (ms) is plotted on the x-axis and amplitude (μV) is plotted on the y-axis.

Bottom Two Panels: N170 ERP waveforms grand averaged and binned horizontally for the memory-guided (MG) and visually-guided (VG) test conditions. The bins are now segmented from left to right, with bin 1 – 4 increasing in ipsilaterally towards the right side, only at the ipsilateral temporal electrode, T6. Time (ms) is plotted on the x-axis and amplitude (μV) is plotted on the y-axis.

Appendix G

Table for Time-Window Mean Amplitudes, Minimum Amplitudes and Latencies (with Standard Deviations) for the Horizontally Binned N170 ERP at T5 (Left Temporal)

Time-Window Mean Amplitude (µV)

	VG	MG	Marginal Mean
Horizontal Bin 1	1.10 ± 6.35	0.59 ± 6.01	0.84
Horizontal Bin 2	1.64 ± 6.34	0.75 ± 5.27	1.19
Horizontal Bin 3	0.69 ± 5.42	0.64 ± 5.65	0.66
Horizontal Bin 4	0.71 ± 5.09	-0.36 ± 4.40	0.17
Marginal Mean	1.03	0.40	

Minimum Amplitude (µV)

	VG	MG	Marginal Mean
Horizontal Bin 1	-1.87 ± 6.07	-2.40 ± 6.53	-2.14
Horizontal Bin 2	-0.79 ± 6.61	-2.12 ± 5.92	-1.46
Horizontal Bin 3	-1.70 ± 5.79	-2.24 ± 6.33	-1.97
Horizontal Bin 4	-1.60 ± 5.29	-3.14 ± 5.28	-2.37
Marginal Mean	-1.49	-2.48	

Latency (ms)

	VG	MG	Marginal Mean
Horizontal Bin 1	202.30 ± 42.83	209.10 ± 38.11	205.70
Horizontal Bin 2	214.70 ± 38.64	211.40 ± 35.13	213.05
Horizontal Bin 3	213.60 ± 30.61	212.10 ± 37.58	212.85
Horizontal Bin 4	212.00 ± 36.64	214.00 ± 39.48	213.00
Marginal Mean	210.65	211.65	

Appendix H

Classical ANOVA Outputs for the Horizontally Binned N170 ERP Measures at T5 (Left Temporal)

Time-Window Mean Amplitude

	df	Error df	F	*p*	η_p^2
Reach Type	1.00	27.00	6.60	.02	.20
Laterality	2.23	60.25	2.38	.10	.08
Reach Type x Laterality	2.81	75.93	1.02	.39	.04

Minimum Amplitude

	df	Error df	F	*p*	η_p^2
Reach Type	1.00	27.00	20.03	< .001	.43
Laterality	2.28	61.64	2.06	.13	.07
Reach Type x Laterality	2.62	70.82	1.34	.27	.05

Latency

	df	Error df	F	*p*	η_p^2
Reach Type	1.00	27.00	0.08	.77	.003
Laterality	2.00	54.07	0.81	.45	.03
Reach Type x Laterality	2.66	71.82	0.40	.73	.02

Appendix I

Table for Time-Window Mean Amplitudes, Minimum Amplitudes and Latencies (with Standard Deviations) for the Horizontally Binned N170 ERP at T6 (Right Temporal)

Time-Window Mean Amplitude (µV)

	VG	MG	Marginal Mean
Horizontal Bin 1	-1.30 ± 4.48	-0.84 ± 4.54	-1.07
Horizontal Bin 2	-1.10 ± 3.72	-0.91 ± 3.94	-1.00
Horizontal Bin 3	-0.21 ± 3.86	-0.24 ± 3.94	-0.22
Horizontal Bin 4	-0.39 ± 3.56	0.05 ± 3.07	-0.17
Marginal Mean	-0.75	-0.49	

Minimum Amplitude (µV)

	VG	MG	Marginal Mean
Horizontal Bin 1	-3.71 ± 6.15	-3.20 ± 5.71	-3.45
Horizontal Bin 2	-3.23 ± 4.72	-3.51 ± 5.96	-3.37
Horizontal Bin 3	-2.72 ± 4.62	-2.59 ± 4.56	-2.65
Horizontal Bin 4	-2.94 ± 4.96	-2.23 ± 3.88	-2.59
Marginal Mean	-3.15	-2.88	

Latency (ms)

	VG	MG	Marginal Mean
Horizontal Bin 1	227.40 ± 54.25	225.70 ± 48.23	226.55
Horizontal Bin 2	230.90 ± 51.75	217.10 ± 46.87	224.00
Horizontal Bin 3	211.30 ± 53.03	221.90 ± 51.75	216.60
Horizontal Bin 4	222.40 ± 53.03	216.40 ± 53.09	219.40
Marginal Mean	223.00	220.28	

Appendix J

Classical ANOVA Outputs for the Horizontally Binned N170 ERP Measures at T6 (Right Temporal)

Time-Window Mean Amplitude

	df	Error df	F	*p*	η_p^2
Reach Type	1.00	27.00	1.72	.20	.06
Laterality	2.45	66.20	4.24	.01	.14
Reach Type x Laterality	2.61	70.51	0.44	.70	.02

Minimum Amplitude

	df	Error df	F	*p*	η_p^2
Reach Type	1.00	27.00	1.17	.29	.04
Laterality	1.78	47.93	2.52	.10	.09
Reach Type x Laterality	1.81	48.87	0.77	.46	.03

Latency

	df	Error df	F	*p*	η_p^2
Reach Type	1.00	27.00	0.30	.59	.01
Laterality	2.91	78.62	0.71	.54	.03
Reach Type x Laterality	2.68	72.44	1.39	.26	.05

Appendix K

VG BIN 1

Time-Window: 150 ms – 300 ms

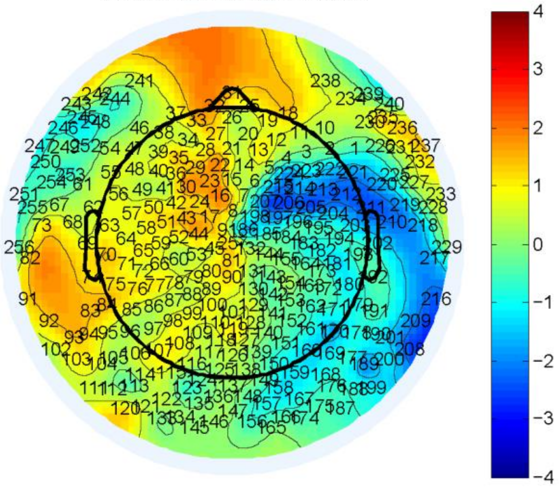

VG BIN 2

Time-Window: 150 ms – 300 ms

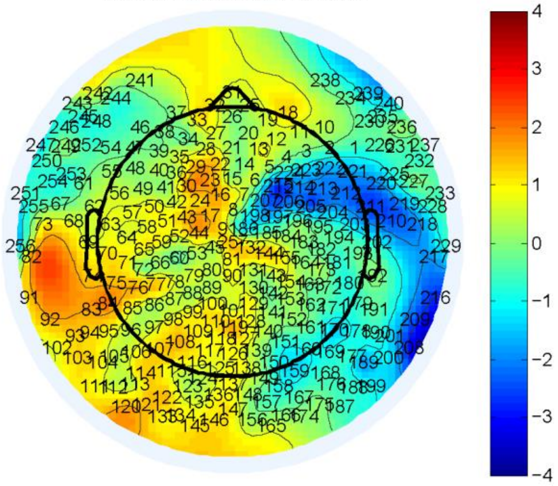

VG BIN 3

Time-Window: 150 ms – 300 ms

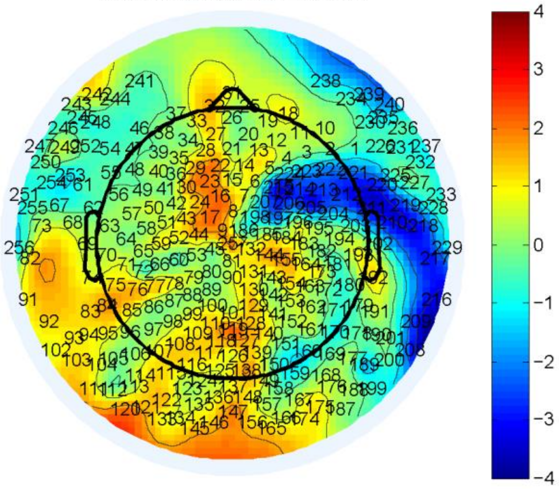

VG BIN 4

Time-Window: 150 ms – 300 ms

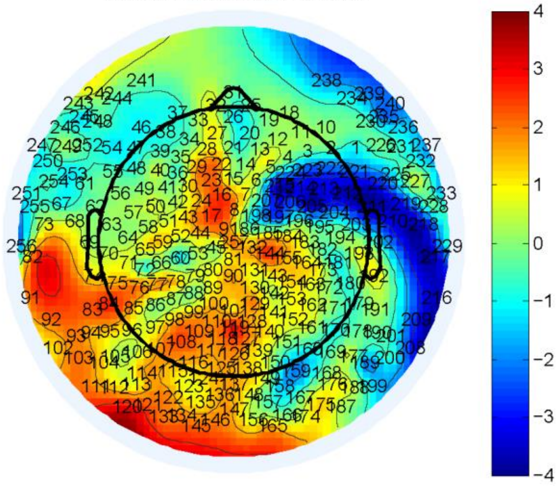

Appendix K Caption:

Topographic plots for the visually-guided (VG) condition, extracted at a time window of 150 ms – 300 ms for all electrodes. The topographic plots are in order from vertical bin 1 – 4, starting from the top left corner to the bottom right corner. Channel numbers 95 and 178, correspond to electrodes T5 and T6, respectively. The color axis on the right-hand side represents voltage (μV) values. Blue represents a negative polarity while red represents a positive polarity. The darker these colors, the higher voltage value.

Appendix L

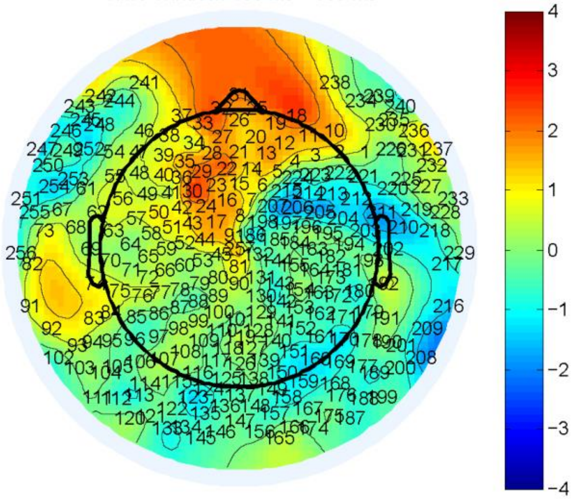
MG BIN 1
Time-Window: 150 ms – 300 ms

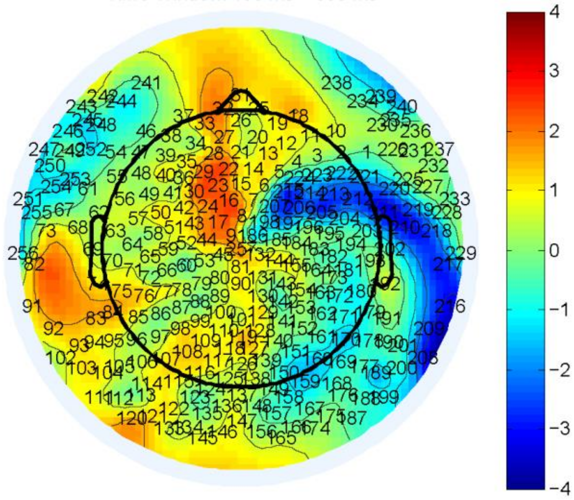
MG BIN 2
Time-Window: 150 ms – 300 ms

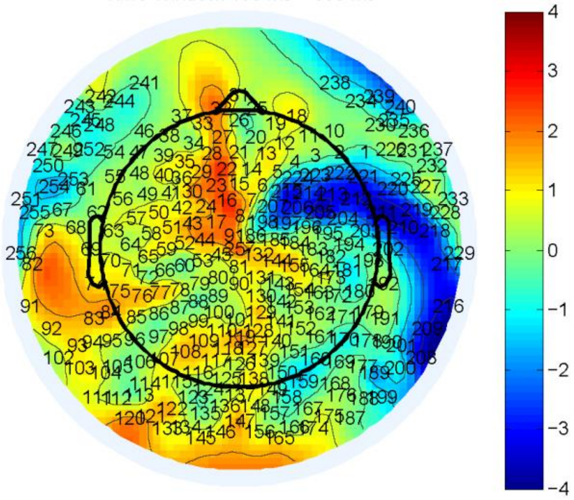
MG BIN 3
Time-Window: 150 ms – 300 ms

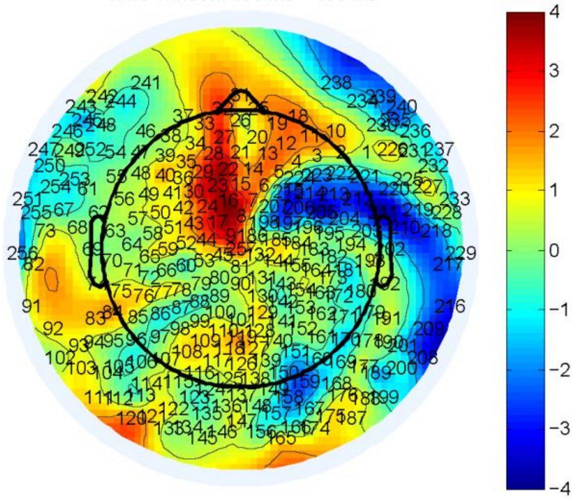
MG BIN 4
Time-Window: 150 ms – 300 ms

Appendix L Caption:

Topographic plots for the memory-guided (MG) condition, extracted at a time window of 150 ms – 300 ms for all electrodes. The topographic plots are in order from vertical bin 1 – 4, starting from the top left corner to the bottom right corner. Channel numbers 95 and 178, correspond to electrodes T5 and T6, respectively. The color axis on the right-hand side represents voltage (μV) values. Blue represents a negative polarity while red represents a positive polarity. The darker these colors, the higher voltage value.